

Soil characteristics and landcover relationships on soil hydraulic conductivity at a hillslope scale: a view towards local flood management.

N. A. L. Archer^{1*}, M. Bonell², N. Coles³, A. M. MacDonald¹, C. A. Auton¹ and R. Stevenson²

¹British Geological Survey, Murchison House, West Mains Road, Edinburgh EH9 3LA, Scotland, UK

²UNESCO Centre, University of Dundee, Perth Road, Dundee DD1 4HN, Scotland, UK

³Centre for Ecohydrology, University of Western Australia, 32 Stirling Highway, Crawley WA 6009, Australia

*Corresponding author: nicarc@bgs.ac.uk

Abstract

There are surprisingly few studies in humid temperate forests which provide reliable evidence that soil permeability is enhanced under forests. This work addresses this research gap through a detailed investigation of permeability on a hillslope in the Eddleston Catchment, Scottish Borders UK, to evaluate the impact of land cover, superficial geology and soil types on permeability using measurements of field saturated hydraulic conductivity (K_{fs}) supported by detailed topsoil profile descriptions and counting of roots with diameters >2mm. K_{fs} was measured at depth 0.04 to 0.15m using a constant head well permeameter across four paired landcover sites of adjacent tree and intensely grazed grassland. The measured tree types were: 500-year-old mixed woodland; 180-year-old mixed woodland; 45-year-old *Pinus sylvestris* plantation; and 180-year-old *Salix caprea* woodland. The respective paired grids of trees and grassland were compared on similar soil texture and topography.

This study highlights the significant impact of broadleaf woodland at a hillslope scale on K_{fs} in comparison to grassland areas: median K_{fs} values under 180-year-old *Salix caprea* woodland (8 mm hour⁻¹), 180-year-old mixed woodland (119 mm hour⁻¹) and 500-year-old Broadleaf woodland (174 mm hour⁻¹) were found to be respectively 8, 6 and 5 times higher than neighbouring grazed grassland areas on the same superficial geology. Further statistical analysis indicates that such K_{fs} enhancement is associated with the presence of coarse roots (>2 mm diameter) creating conduits for preferential flow and a deeper organic layer in the topsoil profile under woodlands. By contrast the *P. sylvestris* forest had only slightly higher (42 mm hour⁻¹), but not statistically different K_{fs} values, when compared to adjacent pasture (35 mm hour⁻¹). In the grassland areas, in the absence of course roots, the superficial geology was dominant in accounting for differences in K_{fs} , with the alluvium floodplain having a significantly lower median K_{fs} (1 mm hour⁻¹) than surrounding hillslope sites, which had a range of median K_{fs} from 21 to 39 mm hour⁻¹.

The data were used to infer areas of runoff generation by comparing K_{fs} values with modelled 15 minute maximum intensity duration rainfall with a 1 in 10 year return period. Infiltration prevailed in the 180 and 500 year old mixed and broadleaf woodland, whereas some grassland areas and the floodplain were inferred to generate overland flow. The significantly higher K_{fs} under deciduous mature forests suggest that the planting deciduous woodlands on hillslopes in clusters or as shelterbelts within grasslands would provide areas of increased capacity for rainfall infiltration and arrest runoff generation during flood-producing storm events.

Keywords: Soil hydraulic conductivity, overland flow, infiltration, flood management, landcover

1. INTRODUCTION

With recent incidents of severe flooding events throughout Northern Europe, flood prevention and mitigation has become a high priority on the public agenda. However, in the context of the current financial crisis, building ever higher flood defences no longer seems to be the way to solve the problem. Instead a combination of restricting development within floodplains and using natural management methods, such as afforestation and wetlands may be a more sustainable way to mitigate future floods (Nisbet and Broadmeadow, 2003). An important criteria in Natural Flood Management (NFM) is understanding and improving the surface soil permeability (or field, saturated hydraulic conductivity, K_{fs} ; Bouwer, 1966; Reynolds et al, 1985; Talsma, 1987) of natural ground surfaces with the view of increasing rainfall infiltration and storage capacity (Bens et al., 2007; Marshall et al., 2009). At the local scale, infiltrability and surface soil permeability (or field, saturated hydraulic conductivity, K_{fs} ; Bouwer, 1966; Reynolds et al, 1985; Talsma, 1987) are key soil properties as they activate surface and near-surface flow paths (Hillel, 1980) that influence runoff generation (Elsenbeer, 2001; Bonell et al., 2010). Such soil hydraulic properties control *dominant* storm flows (defined in Chappell et al., 2007) and can provide preliminary understanding of runoff generation when linked with rainfall characteristics (Bonell and Bruijnzeel, 2005).

As noted by Chandler and Chappell (2008), there is a general acceptance that permeability of forest soils is higher than that of soils supporting other vegetation types, but their review of the scientific literature revealed that there are surprisingly few studies that test this hypothesis. Such remarks apply in particular to humid temperate forests as in recent times there has been an escalation of such work in the tropics (Deuchars, et al., 1999; Elsenbeer, et al., 1999; Bonell, 2005; Germer, et al., 2010; Bonell, et al., 2010; Hassler, 2011) linked with the extensive forest conversion since the mid- 20th Century (Drigo, 2004; 2006). These

studies suggest that trees overall enhance permeability, but there are also exceptions, as reviewed in Chandler and Chappell (2008) and elsewhere (Bonell et al., 2010; Ghimire et al., 2013).

The few studies that have been done in temperate areas suggest that forests have higher infiltration rates and also near-surface, field saturated hydraulic conductivities than grassland cover, because of enhanced incorporation of organic matter from litter fall, a greater diversity of soil fauna, as well as higher root densities and root diameters; all of which in turn, enhance soil macroporosity and soil structure (Beven and Germann, 1982; Alaoui et al., 2011; Schwärzel et al., 2012). It has also been found in a small French catchment study that land use had a significantly greater impact on K_{fs} than differences within pedologic units and the highest K_{fs} values were associated with broad-leaved forests and small woods rather than pasture land (Gonzalez-Sosa et al., 2010). Older forest stands have also been found to have higher rates of K_{fs} than recently planted trees (Leiva et al., 2009 and Hümman, et al., 2011) or adjacent agricultural areas (Peng et al., 2012).

Forested areas however, do not always give higher K_{fs} values. Investigations of soils under recent afforestation have shown that the upper soil layers still possess physical conditions and similar runoff formation processes of the former agricultural soils (Bonell et al., 2010; Hümman et al., 2011, Krishnaswamy et al., 2012). Soil acidification from the decomposition of acidic litter, particularly in conifer plantations can lead to reduced soil structural ability (e.g., collapse of soil aggregates) and thus reduced macro-porosity (Chappell, 1996).

Moreover microbial soil activity can cause hydrophobicity in soil macropores, thus reducing soil permeability (Morales et al., 2010). Factors which cause soils to be hydrophobic are viewed negatively for rainfall infiltration. On the other hand, in south- east Australia, Nyman

et al., (2010) suggests a synergy between effect of macropore flow and water repellency, where water repellency induces ponding at increasing scale, activating flow through macropores, which then raises effective infiltration rates at larger scales.

Planting trees on degraded land is not sufficient in itself to restore the permeability and hydrological functions of degraded catchment areas, but management of forests is also important. For example, Ghimire, et al. (2013) found that repeated collections of litter from the forest floor supplemented by continuous cattle grazing in community forests in Nepal caused a reduction of soil organic matter that could not be incorporated into the soil to form larger soil pore networks. This caused a decrease in permeability in the upper 0.25 m soil depth.

The preceding discussion shows that natural processes of soil permeability which develops under forestation is complex. Moreover there are practical implications. For example when implementing NFM as an approach to flood risk management particularly at a legislative level such as , the Flood Risk Management (Scotland) Act 2009 (Scottish Government, 2009), it is very important, to better understand the dynamic relationship of hydraulic conductivity developed under forests of different species and ages.

1.1. Scope and aims of the work

The study will therefore evaluate *in situ* K_{fs} measurements taken at the soil surface and below ground (either to 0.15m or 0.25m depth) at sites across a range of superficial geology and soil types (previously glaciated); and land cover of adjacent grazed grassland and woodland cover linked with an experimental transect in the Eddleston catchment. The tree cover areas include old-growth remnant broadleaf woodland; a 180 mixed broadleaf/conifer woodland, a 45 year old pine plantation; and a mature willow woodland within a riparian

wetland. In addition, improved grazed grassland adjacent to woodland areas on both a hillslope transect and within a floodplain are considered. The K_{fs} survey should be considered as 'snapshots' in time as it is well known since the 1980s (e.g., Gish and Star, 1983; Bonell and Williams, 1986) that temporal variability of K_{fs} at a point can be statistically significant as is spatial variability.

The primary aim of the work:

- i. is to evaluate the impacts of superficial geology and soils *vis-a-vis* land cover on K_{fs} . Such steps are intended to indicate possible differences of K_{fs} between grassland and different types of woodland of different ages, and thus contribute towards a better understanding of the positive and negative impacts of forest on K_{fs} , in response to Chandler and Chappell (2008). This work will be supported by detailed soil descriptions including some root characteristics.

Additional aims of the work:

- ii. Subsequently in the absence of hillslope hydrology experimentation, some consideration will be given to whether infiltration-excess overland flow (Chorley, 1978) can be inferred, or not, over specific land covers linked with intensity-frequency-duration (IDF) developed for the experimental area. For a limited number of sites, the possible occurrence of other stormflow pathways (i.e., using the definitions of Chorley, 1978) will also be briefly considered where K_{fs} data are available for two soil depth ranges (i.e., 0-0.15m, 0.15-0.25m).
- iii. Finally some consideration will be given to possible contributions of the work in the context of Natural Flood Management.

2. EXPERIMENTAL SITE

2.1. Location

The site is located on a hillslope that has an altitudinal range from 192 m to 255 m above Ordnance Datum (OD) with a slope gradient varying from 1 to 22 %. The field area is approximately 0.5 km² and extends to the floodplain of the Eddleston Water, a tributary of the River Tweed in the Scottish Borders (55°42.9'N, 3°13'W). It is within the Eddleston Water monitoring catchment, which has been established to assess the effectiveness and efficiency of NFM (Fig. 1).

2.2. Historical land cover

The environmental evolution of the site area is typical of much of the Scottish Borders. Analysis of pollen samples, taken from an area to the north of the catchment, (Ashmole and Tipping, 2009) suggests that the region was well wooded at the Holocene 'climatic optimum', around 6800 to 4800 years ago. These woods were dominated by *Alnus*, *Ulmus*, *Fraxinus* and *Quercus*, with *Sorbus*, *Crataegus*, *Populus*, *Ilex* and *Prunus* as minor components. Most of the trees were removed to create the grazing needed to sustain increased stocking levels that began during Medieval times (Ashmole and Tipping, 2009). This mainly pastoral landscape has been maintained to the present day. Today forestation is biased towards fast growing conifer species as shown by the National Inventory of Woodlands and Trees, where most forestation in recent times in the Scottish Borders has been dominated by conifer woodland and represents about 78% of all woodland area (Anon, 1999). For the remainder "...broadleaved woodland represents 7%, mixed woodland 3% and open space within woodlands 9%" (Anon., 1999, p. 2).

2.3. Soils and geology

According to the Soil Survey of Scotland Map (Scotland Soil Survey Staff, 1975), the site is dominated by two soil associations; Yarrow soils on the hill slope and Alluvium on the floodplain. The Yarrow association, which are classified as Cambisols (WRB, 2006), comprise brown forest soils developed on gravels that are mainly derived from weakly metamorphosed argillaceous sandstones (greywackes). A subsequent more detailed field survey of the superficial geology and morphology of the study site (and its surroundings) was undertaken by Ó Dochartaigh et al. (2012). Using the soil classification of the Soil Survey of Scotland (Bown and Shipley, 1982), the survey indicated that this Yarrow association (Cambisols) could be further subdivided into two series in some areas based on drainage. Thus some areas were not so freely draining and tended to be more closely related to the Kedslie soil series, while other areas were more freely draining except for some gleying and were more closely related to the Linhope soil series. The alluvial soils (known as Fluvisols in the WRB classification, 2006) are developed on relatively recent freshwater sediments that mainly comprise mixtures of silt, with varying amounts of sand and clay; fine- to coarse-grained gravels are present as subordinate components throughout their soil profiles.

The above mentioned work of Ó Dochartaigh et al. (2012) included the production of a 1: 25 000 scale map of the superficial geology and landforms of the whole catchment, between Penicuik and Pebbles (British Geological Survey, 2011). The site area is underlain by Ordovician meta-sandstones of the Portpatrick Formation that are typical of this part of the Scottish Borders. These rocks comprise brittle but resistant strata which crop out near to the surface of the soil on parts of the hillslope.

Six superficial (unlithified) geological units occur in the field area, as shown in Fig. 2. First, 'Head' or colluvium, is the most widespread. It is typically a 'gravelly' sediment, derived from

underlying materials (commonly bedrock or glacial till) by solifluction, creep and slope wash and produces poorly sorted stony soils. Second, 'glaciofluvial ice-contact deposits' are sediments that were laid down at the margin of the last (Late Devensian) ice sheet as it retreated across the area, some 15, 000 to 13, 000 years ago. They comprise thick accumulations of sand and gravel that occupy the valley floor now drained by the Eddleston Water and, within the floodplain, they are mantled by later Holocene alluvial sediments. Similar 'ice-contact deposits' also form gravel mounds that blanket much of the western side of the valley upstream and downstream of the study transect. Here, they produce well drained gravelly soils. Glacial meltwater drainage also created a ravine (the Fairy Dean), largely cut into bedrock, to the south of the site. These meltwaters also laid down the 'glaciofluvial sheet deposits' (third superficial geological unit) of finer-grained sand and gravel within the ravine, upon which sandy soils developed.

As the fourth superficial geological unit, glacial 'till' is widely developed, mantling bedrock on many of the valley sides in the catchment, but only a single surface exposure is present within the slope transect. However, geological modelling and geophysical profiling (Ó Dochartaigh et al., 2012) indicate that this compact, silty, gravelly material is widespread beneath the 'head' and 'ice-contact deposits' on the hillslope. 'Alluvial' deposits (fifth unit) are dominant beneath the floodplain, where they comprise fine-grained material, mainly silt (formed as overbank deposits during flooding events) as well as beds of coarse gravel and sand that were laid down by laterally migrating river channels. The final sixth geological unit is an area of shallow 'peat' which is present near the western side of the river, where a sedge plant community is present and drainage is poor. Similar humic units commonly occur as lenses at depth, interbedded within the sandy and silty alluvial sediments.

3. METHODOLOGY

3.1. Locating K_{fs} grid areas within the hillslope and floodplain

To test whether land cover causes a significant difference to K_{fs} , it was essential that the chosen areas with different land covers were located in areas with the same parent material. As the more recent superficial geology survey and resulting map (British Geological Survey, 2011; Ó Dochartaigh et al., 2012;) better reflected the spatial differences of soil characteristics than the older soil survey map (Soil Survey of Scotland Staff, 1975), then the former was used to locate land cover pairs (i.e. grassland and woodland). Detailed selection of the grids was also based on a combination of position on the hillslope and floodplain (i.e. ensuring that they were located within the same contour line, as shown in Fig. 1) as well as the location of the same superficial geological unit (Fig. 2).

Fig. 1. Aerial Photo and cross-section of the field study site, showing Site 1 which contains Site 1 grazed grassland (G1) and 500 year old broadleaf woodland (DW1) situated at the top of the slope, site 2 contains grazed grassland (G2) and 180 year old broadleaf woodland (DW2) located on a relatively flat part of the slope, site 3 containing grazed grassland (G3) and 45 year old conifer plantation (CW3) is on the steepest part of the slope and site 4 is located on the floodplain and contains floodplain woodland (FW4) and grazed grassland (G4).

Fig. 2. Superficial geology of study area, showing the eight areas of K_{fs} measurements. Black lines are 10 m contour lines and open white areas are rock outcrops occurring within 1 m of the soil surface. G1 is grazed grassland, DW1 is 500 year old broadleaf woodland G2 is grazed grassland, DW2 is 180 year old broadleaf woodland, G3 is grazed grassland and CW3 is 45 year old conifer plantation FW4 is floodplain woodland and G4 is grazed grassland.

In this way four sites were chosen containing two different land covers, i.e. grazed, improved grassland cover and tree cover at different altitudinal locations (Fig. 1). All grassland areas were heavily grazed by cattle and/or sheep between early spring in April and autumn. A study of historical maps covering the area suggests that all the existing grassland has been

under this land cover for at least 250 years. All wooded areas were fenced and protected from grazing. The descriptions of sites are:

- Site 1 has a slope from 0 to 5% and is located on the highest slope (elevation 250 m OD) of the site area. It includes an area of improved grazed grassland (G1) and old remnant woodland dating back to 1536, when Barony Castle was built and set in 10 hectares of broadleaf woodland (DW1). The woodland area contains mature trees, comprising *Fagus sylvatica*, *Prunus spinosa*, *Quercus petraea*, *Betula pendula*, *Acer pseudoplatanus* and a few *Fraxinus excelsior* and *Pinus sylvestris* randomly spaced from 3 to 15 m.
- Site 2, lower down the slope (elevation 240 m OD), includes an area of improved grazed grassland (G2) and a mixed woodland (DW2), that is part of the Barony Estate, and has been partially felled during the last 180 years. The slope ranges from 0 to 10%. The woodland in DW2 is randomly spaced from 3 to 20 m and is more mixed than DW1 with *P. sylvestris* and there are fewer *F. sylvatica* present.
- Site 3 is on the steepest part of the hillslope (between 5 to 22 % slope). It ranges in elevation from 230 to 210 m OD and contains improved grazed grassland (G3) and part of a 45-year old *P. sylvestris* plantation (CW3). G3 and CW3 are separated by a topographical depression (as shown in Fig. 1). The trees in CW3 were planted by hand in lines 1 to 5 m apart.
- Site 4 is on the floodplain (0 to 2% slope), at 197 m OD. It is divided into improved grazed grassland (G4), and a small area of wetland dominated by *Salix caprea* (FW4) randomly growing together as a small clump of woodland.

A sampling grid was established in each of these eight areas to position the *in-situ* permeability measurements. Depending on the size of area being evaluated, individual grid cells ranged in size from 4 m² to 625 m². In order to avoid edge effects, caused by land cover changes, the edge of all grids were placed a minimum of 5 m inside of the margin of each land cover type. A summary of site characteristics, site area, sampling grid size and soil measurement depths are given in Table 1.

Table 1) Site description, grid sampling size, and K_{fs} measurement depths. G1 is site 1 grazed grassland, DW1 is 500 year old broadleaf woodland G2 is site 2 grazed grassland, DW2 is 180 year old broadleaf woodland, G3 is site 3 grazed grassland and CW3 is 45 year old conifer plantation FW4 is floodplain woodland and G4 is site 4 grazed grassland.

3.2. Measurement of hydraulic conductivity (K_{fs})

3.2.1. The Constant Head Well Permeameter

A hole was augered within 1 m of each grid intersection and the soil depths and numbers of sample points (i.e. grid intersections) are given in Table 1. K_{fs} was measured using a constant head well permeameter (CHWP) as designed by Talsma and Hallam (1980). A stony layer below 0.15 m at sites G2, W2, G3, and W3 restricted augering below 0.15 m. To ensure a comparative data set across all grid areas, the auger hole depth was therefore set to 0.15 m for all sites. To avoid interaction of the soil surface on the steeper slopes, the constant falling head level was set to 0.04 m below the soil surface, thus providing a head (h) of 0.11 m for all measurements at soil depths 0.15 m. In grid areas G1, W1 and G4, it was possible to auger to 0.25 m. Therefore, for these sites a second hole was augered within 1 m of a sample point and a CHWP measurement was taken from 0.15 m to 0.25 m. A 0.06 m diameter auger was used throughout the investigation. The auger hole radius (a) was generally between 0.0325 to 0.035 m. This gave an H/a value of approximately 3. To reduce the problem of smearing the wall of the auger hole during augering, a stiff nylon brush was

used to gently brush the auger hole walls (McKay et al, 2005). A pre-wetting phase of 20 minutes was then carried out before starting the permeameter test. This reduced the time to reach steady state flow and ensure that each measured point was saturated (Talsma and Hallam, 1980).

In the floodplain, the water table in some areas was found to be within 0.2 m of the ground surface, therefore the grassland grid area was located where the water level was deeper than 0.6m at the time of K_{fs} measurements. In the floodplain woodland, the cavities were augered to a maximum depth of 0.15 m, because the water table was rarely deeper than 0.5 m.

Following a comparative study of CHWP formulae, as described elsewhere (Archer et al., 2013), the Glover solution with a correction for the effect of gravity (Reynolds et al., 1983), was chosen to be the best solution to estimate K_{fs} .

3.2.2. The Poned disc permeameter

K_{fs} was measured using the ponded version of disc permeameter (PDP), as designed by Perroux and White (1988) at only DW1 and G4, because the topography at other sites were insufficiently level to take measurements. An initial soil core was taken and weighed in the field before measurements commenced. Following each PDP measurement, surface water was allowed to drain from the soil surface, and then a sample from the top 5 mm of soil was removed. These soil samples were taken to the laboratory and the volumetric water content for each soil sample was estimated using gravimetric procedures. Measurements commenced the moment the ponded reservoir in the PDP had filled, and in this way the soil sorptivity could be measured, as described by Coughlan et al. (2002). Measurements were

taken until steady state infiltration was achieved and K_{fs} was calculated using equation 1 (White and Sully, 1987).

$$K_{fs} = q/\pi r_0^2 \frac{4bS_0^2}{\pi r_0(\theta_0 - \theta_n)}$$

Equation: 1

Where $q/\pi r_0^2$ is steady state flow (mm hr^{-1}) and is calculated from the slope of the linear portion of cumulative infiltration against hours; b is a constant (0.55); S_0 is sorptivity; calculated from the initial linear slope of $Q/\pi r_0^2$ against hours $^{1/2}$; r_0 is the radius of the metal ring where water infiltrates directly into the ground; θ_0 is the initial volumetric moisture content before the start of measuring and θ_n is the final volumetric moisture content at the soil surface after the measurement has finished.

The location of measurements followed the same grid system as the CHWP measurements so that the K_{fs} values could be compared to the same locations of K_{fs} measurements.

3.2.3. Soil descriptions for each grid area

For each hole augered for the CHWP measurements, soil descriptions of soil horizons were noted and included soil colour, depth of organic horizons and gravel size (including depths of gravel layers). Gravel was categorized using the British Standard range of particle sizes (British Standards Institution, 1990) into fine gravel (2 to 6 mm), medium gravel (6 to 20 mm) and coarse gravel (20 to 60 mm). The auger holes were divided into 0.05 m increments to a depth of 0.15 m and presence of fine roots ($\geq 2\text{mm}$) were noted. Any roots above 2 mm were counted into two categories 2 to 5 mm, and >5 mm for 0.05 m soil depth increments. In this way, each K_{fs} measurement related to a soil profile description, number of gravel size and

root size which allowed regression analysis to compare possible statistical associations of K_{fs} values against gravel size as well as root characteristics.

Bulk samples were collected, from four auger holes in each grid area, for particle-size analysis. The latter was undertaken by dry sieving the material > 2 mm diameter; the particle size distribution of material < 2 mm was measured using a Beckman and Coulter LS13 320 Laser Diffraction Particle Size Analyzer.

3.3. Data analysis

3.3.1. Geostatistical analysis: test for autocorrelation between K_{fs} values

To test for significant differences of K_{fs} between grid sites, the data for each grid was first checked for autocorrelation using Ordinary Kriging in ESRI® ArcMap™ 9.3.1. Generally at shallow depths at sample locations (lags) of 25, 10, 1 and 0.25 m, K_{fs} has been found to have little to no spatial structure in other studies, as discussed by Sobieraj *et al.* (2004). To investigate such possible spatial structure at smaller scales, five extra sampling points were nested within the grassland and woodland grid areas, at lags 0.25, 0.5, 1, 3 and 5 m, within site 1 following the sampling methodology of Zimmermann and Elsenbeer (2008). The strength of spatial variability was estimated using the ratio of nugget to sill (total semivariance), which provided a percentage to classify spatial dependence using the following criteria : <25% indicates strong spatial dependence, between 25 and 75% indicates moderate spatial dependence and >75% indicates weak spatial dependence (Cambardella *et al.*, 1994). Using an exponential Simple Kriging model, strong autocorrelation was found to exist at a range within 2 m in the grassland and woodland area at site 1. Taking into account this result, the chosen grid points (distance between K_{fs} sampling points) for all sites were significantly greater than 2 m apart and thus ranged from a minimum of 2.5 m to 25 m, as shown in Table 1.

3.3.2. Statistical analysis

Using the Anderson-Darling and Kolmogorov-Smirnov statistical tests for normality, it was determined that K_{fs} values measured in all the grass areas and the floodplain woodland (FW4) were log normally distributed. The data was therefore transformed using \log_{10} before further analysis, which is common for such datasets (Bonell et al., 2010; MacDonald *et al.*, 2012). All transformed K_{fs} values for each grid area was tested for homogeneity of variance using Bartlett's test.

To determine significant differences of $\log_{10} K_{fs}$ values between paired grid areas (which had normally distributed data and equal variances), paired t-tests were used. Where mean variances were not similar, the nonparametric equivalent of the paired t-test that is, the Wilcoxon's signed rank test was adopted using the procedure of Dytham (1999, p. 76).

To test the null hypothesis that all site locations (Sites 1 to 4) have the same mean under grassland and woodland, one-way ANOVA was used if the grid area K_{fs} was normally distributed and had equivalent mean variances. If the mean variances were unequal, the Kruskal-Wallis non-parametric test was used. If the ANOVA gave a significance difference, the data was further interpreted using descriptive statistics and Fisher's Least Significant Differences to determine which of the grid locations had the most significantly different K_{fs} values.

3.3.3. Rainfall intensity-duration-frequency analysis (IDF) and inferring dominant hillslope hydrological pathways during storms

There are an increasing number of studies particularly in the tropics and subtropics suggesting that the vertical distribution of K_{fs} and prevailing rainfall intensities are driving factors that determine the dominant stormflow pathways (as defined by Chappell et al, 2007) during and shortly after a rainfall event (Gilmour et al., 1987; Ziegler et al., 2006;

Zimmermann and Elsenbeer, 2008; Germer et al., 2010; Bonell et al., 2010; Hassler et al. 2011; Chandra et al., 2013). All these investigations infer stormflow pathways (e.g., infiltration – vertical percolation, infiltration –excess (IOF, Horton, 1933) or saturation-excess (SOF) overland flow, subsurface stormflow, SSF; Chorley, 1978) by selecting percentiles of maximum rainfall intensities (I_{\max}), which are then superimposed on measured datasets of K_{fs} values.

In this study I_{\max} for different rainfall durations for the field site were derived using the Flood Estimation Handbook (FEH) depth-duration-frequency (DDF) model on a 1 km grid, as described by Faulkner (1999) to fit rainfalls aggregated over 15 to 360 minute rainfall durations for 2, 5, 10, 20 and 100 year return periods (Fig. 3). The rainfall database spanned at least 10 years and used local rainfall gauges within 8 km of the study area. The values modelled for DDF curves, 1 in 2, 5, 10, 50 and 100 year return periods over $I_{15\max}$ were converted to rainfall intensity-duration–frequency (IDF) values and then superimposed on boxplots to illustrate the spread of K_{fs} values for each measured grid area. The choice of $I_{15\max}$ of different return periods was to conceptualize how short–duration, high intensity storms may cause IOF in relation to the range of measured K_{fs} under different land cover. As K_{fs} was measured at several depths (soil surface, 0.04-0.15m and 0.15-0.25m) at sites 1 and 4, thus the possible inference of subsurface stormflow (SSF) could also be considered at these sites, as described by Bonell (2005).

Fig. 3 Modelled DDF curves using the Flood Estimation Handbook (Faulkner, 1999) aggregating rainfalls over 15 to 360 minute rainfall durations for 2, 5, 10, 20 and 100 year return periods.

4. RESULTS

4.1. Comparison of K_{fs} values

4.1.1. K_{fs} between different land covers at 0.04 to 0.15 m depth.

The K_{fs} values measured between depths 0.04 and 0.15 m for each grid area are displayed in Fig. 4 and also graphed as a box plot (Fig. 5) to illustrate the spread of data and the median for each grid area. The oldest forest area (DW1) shows the highest range of K_{fs} values (60 to 482 mm hr⁻¹) than any other grid area, whereas the floodplain (G4) shows the lowest range of K_{fs} values (0.4 to 12 mm hr⁻¹).

Fig. 4. Spatial display of K_{fs} measured points within each grid area. Grid areas are identified as abbreviations and contour lines are shown as black full lines, ranging from 210 m to 260 m. G1 is grazed grassland, DW1 is 500 year old broadleaf woodland G2 is grazed grassland, DW2 is 180 year old broadleaf woodland, G3 is grazed grassland and CW3 is 45 year old conifer plantation FW4 is floodplain woodland and G4 is grazed grassland. Grid areas G1, DW1 and FW4 are enlarged to show the K_{fs} categories more clearly.

Fig. 5. Box plots of measured K_{fs} for each field site measured between 0.04 to 0.15 m soil depth. K_{fs} median values are given in the table. The superimposed black and dashed lines I_{15max} rainfall intensity events for selected return periods of 1 in 2 years (22.0 mm hr⁻¹), 1 in 5 years (29.8 mm hr⁻¹), 1 in 10 years (36.3 mm hr⁻¹), 1 in 50 years (56.4 mm hr⁻¹) and 1 in 100 years (68.0 mm hr⁻¹).

Highly significant differences between tree cover and grassland areas were found for all sites, except between G3 and CW3 (Table 2). The median K_{fs} values in the grid areas DW1, DW2 and FW4 are respectively 5, 6, and 8 times more than the corresponding adjacent grass areas. Such characteristics can be seen in the extreme values between grass and woodland areas, as shown in Fig. 4 and 5, and the means and standard error given in Table

2. In summary the rank of median K_{fs} for the 0.04 to 0.15 m soil layer is DW1 > DW2 > CW3 > G1 > G3 > G2 > FW4 > G4.

Table 2. Results of the paired t-test and Wilcoxon's test, which compare the differences between the tree and grassland grid areas within each site. SE of mean is the standard error of the mean, *** indicates highly significant differences between the grid areas within each site. G1 is site 1 grazed grassland, DW1 is 500 year

old broadleaf woodland G2 is site 2 grazed grassland, DW2 is 180 year old broadleaf woodland, G3 is site 3 grazed grassland and CW3 is 45 year old conifer plantation FW4 is floodplain woodland and G4 is site 4 grazed grassland.

4.1.2. A comparison of K_{fs} within grassland and woodland areas at the 0.04-0.15m depth

One-way ANOVA \log_{10} transformed K_{fs} values showed very highly significant differences between the grassland sites (G1, G2, G3 and G4) (F ratio = 97.7, d.f. = 3 and P value < 0.001). Fisher's Least Significant Difference showed that the most significantly different (P < 0.05) grassland area was in the floodplain (G4), where the median K_{fs} value of G4 was between 17 and 33 times lower than the respective mean K_{fs} values for G2, G3 and G4 (also shown as mean values in Table 2 and Fig. 4). During the summer when stocking densities were high, it was observed that in the floodplain the soil surface became pitted with hoof prints and during high intensity rainfall, surface- ponding occurred.

The Kruskal-Wallis nonparametric test was used to test for significant differences between woodland areas (DW1, DW2, CW3 and FW4). The results showed that the K_{fs} values were very high significantly different for the four woodland areas (H-value = 26.19, d.f = 3 and P value < 0.001). Summary statistics and the box plot (Fig. 5) suggest that the highly significant differences lie between CW3 and FW4, which have much lower K_{fs} values than DW1 and DW2.

4.1.3. A comparison of K_{fs} where measurements were made at three different soil depths (soil surface, 0.04-0.15 and 0.15-0.25m) for DW1, G1 and G4.

The spread of K_{fs} values are illustrated as box plots (Fig. 6) for the three grid areas for each measured soil layer. The surface soil K_{fs} measurements using the PDP are shown for grid areas G4 and DW1 and K_{fs} values for the soil layers 0.04 to 0.15 m and 0.15 and 0.25 m, were measured by CHWP method.

One-way ANOVA was used to investigate significant differences of K_{fs} between soil layers.

The results are shown in Table 3 and include mean K_{fs} and standard error values for each grid and soil depth. Very highly significant reductions of K_{fs} are indicated with increasing soil depth, particularly below 0.15 m in DW1 and G1. In G4 the 0.04 – 0.15 m soil layer has the lowest K_{fs} values, whereas the deeper layer has higher K_{fs} values.

Fig. 6. Box plots of measured K_{fs} for DW1, G1 and G4 at three different soil depths: 0 m, 0.04 – 0.15 m, 0.15 – 0.25 m. The superimposed black and dashed lines are I_{15max} rainfall intensity for selected return periods of 1 in 2 years (22.0 mm hr⁻¹), 1 in 10 years (36.3 mm hr⁻¹) and 1 in 100 years (68.0 mm hr⁻¹).

Table 3. Results of one-way ANOVAs, comparing $\log_{10} K_{fs}$ values for different depths for each grid DW1, G1, G4. *** means that the P-value is very highly significant and ** means the P-value is highly significant. The table also includes the mean and standard error (SE) of K_{fs} values for each soil layer. G1 is site 1 grazed grassland, DW1 is 500 year old broadleaf woodland and G4 is site 4 grazed grassland.

4.2. Soil and root characterisation of grid areas

The auger hole soil profiles showed that the main differences in the topsoil (0 to 0.3 m) between different grid areas are the depth of gravel and organic layers within this upper surface soil profile. These differences are shown as simplified surface soil profiles in Fig. 7, using the horizon nomenclature from the Soil Survey of Scotland Handbook (Macaulay Institute for Soil Research, 1984). The shallow soil survey found that fine to coarse gravels came to the surface in some areas on the steep hillslope section within CW3 and G3. The gravel layer was deeper in DW1 and G1 (below 0.25 m) than DW2 and G2. Gravel was also found in a very few patches within the floodplain (FW4 and G4).

Soil particle size analysis of the < 2 mm fraction indicated that the silt and clay fraction increases downslope onto the floodplain at G4 and FW4 and the sand fraction increases upslope, and is the highest in DW1 and G1 (this is illustrated in Fig. 8).

The deeper organic layers under all woodlands were a sharp contrast with the adjacent grassland areas, the latter of which were characterised as having a 40 to 50 mm dense root mat comprised of fine roots less than 2mm diameter (see Fig. 7). The vertical profiles of these broadleaf woodland soils indicated a high level of biological activity, because of the presence of a large number of tree and shrub roots and a deep organic layer. The deepest organic layer was in DW1 and was shallower in the conifer plantation (CW3). DW2 had a thinner organic layer and a shallower A horizon than DW1.

Table 4. Generalised soil descriptions and their relationship with the superficial geology for all grid areas.

Large mature tree roots (diameters > 5mm) were found close to trees in all wooded sites (DW1, DW2 CW3 and FW4). The coarse root counts in Fig. 7, show that DW1 had the largest number of coarse roots (classified between 2 to 5 mm and >5 mm) than any of the other grid areas. Also the distribution of these coarse roots in DW1 was more homogenous at depth in comparison to DW2 and CW3, where coarse roots decreased at 0.15 m. In the floodplain woodland (FW4), the 2 to 5 mm roots were highly clumped and found mainly in the top 0.10 m of the soil. Within the grass areas the 0 to 0.05 m soil depth was dominated by a thick grass root mat. No coarse roots (>2mm) were observed in the soil profiles in the grass areas.

Fig. 7. The graphs in the row labelled 'roots', show the number of coarse roots within a soil profile. The y axis is soil depth (cm) and the x-axis is the number of coarse roots; the black bar indicating average number of roots with diameters between 2 to 5 mm and the grey bars indicating number of roots > 5 mm. Error bars show the standard error for each grid area. The row labelled ' K_{fs} ' shows the K_{fs} (mm hr⁻¹) for each sampled point within each grid. The row labelled 'soil' shows the soil profile from 0 to 0.25 m for grid areas G1, DW1 and G4 and RW1, all other profiles are for soil depths 0 to 0.2 m. The L horizon is fresh annual litter, the F horizon is decomposed litter, H is well decomposed matter under aerobic conditions, A is a mineral horizon incorporating organic matter, B is a mineral horizon and C is a mineral layer of unconsolidated material. The black fragments indicate the depth of coarse gravels.

Fig. 8. Average percentage clay, silt and sand measured for each grid area.

4.2.1. Relationship of K_{fs} versus gravel content and presence of roots

The K_{fs} values higher than 120 mm hr^{-1} all had roots $>5 \text{ mm}$ present within the auger hole (Fig. 9). Regression analysis was used to test correlations of K_{fs} measured from 113 auger holes and their corresponding soil descriptions which contained, total root numbers, number of roots $>5 \text{ mm}$, number of roots between 2 and 5 mm, humus depth, gravel size, depth of gravel layer. As shown in Fig. 9a, analysis using logarithmic regression gave positive 52% correlation (R^2) between K_{fs} values and total root numbers $>2 \text{ mm}$ diameter ($F = 41.82$, P -value < 0.001). On the other hand using regression analysis, no correlation was evident between gravel size (Fig. 9b) and K_{fs} . Using Minitab version 16.2.3 best subset regression showed that the inclusion of additional independent variables (i.e., humus depth, stone size total root size) with total root numbers $>2\text{mm}$ did not greatly improve R^2 and thus the prediction of K_{fs} . For example, the additional inclusion of humus depth, and stone size with total root numbers $>2\text{mm}$ into the best subset regression predicted only an increase of 5% in R^2 , i.e., from 50% to 55 % of the K_{fs} values. This analysis corroborates the results of MacDonald et al. (2012), who found that $\log K_{fs}$ had a low correlation to material descriptions using the largest fractions (e.g. sand or gravel).

Fig. 9. a) K_{fs} for all auger holes versus number of coarse roots ($>2 \text{ mm}$). The linear regression line is: $K_{fs} = 25.94 - 3.434\text{roots} + 1.482 \text{ roots}^2 - 0.03648\text{roots}^3$. $P < 0.001$ and R^2 is 52.2%. b) K_{fs} for all auger holes versus maximum gravel size. No statistical significance ($P = 0.891$ and R^2 is -0.88%).

4.3. Rainfall intensity-duration-frequency (IDF) analysis for different land covers

Fig. 5 illustrates that the range of K_{fs} values of the oldest woodland (DW1) and 180 year old mixed woodland (DW2) exceeds I_{15max} events for 1 in 100 year storm events. On the other hand the upper quartiles of K_{fs} values in all grazed grassland areas are below the I_{15max} , 1 in 100 IDF. Further the whole range of K_{fs} values remains well below the I_{15max} , 1 in 10 IDF in G2, and for the paired floodplain sites G4 and FW4. Such features infer that the grassland areas and particularly the floodplain will have infiltration-excess overland flow occurring during such storm events.

Where it was possible to measure K_{fs} at 0.15 to 0.25 m soil depths (i.e., at DW1, G1 and G4), it was found that the range of K_{fs} values were much lower in this layer when compared to the <0.15m depth (as shown in Fig. 6). Such reductions in the 0.15 – 0.25m layer were particularly marked under the woodland area (DW1) where K_{fs} ranged from 8 to 51 mm h⁻¹, i.e., by up to 2 orders of magnitude when compared to the K_{fs} <0.15m depth. Thus during I_{15max} for both 1 in 100 and 1 in 10 IDF, impedance to percolation is indicated and thus will lead to subsurface stormflow particularly within DW1.

Fig. 6 also shows that within the floodplain all soil layers are highly impermeable, because the range of K_{fs} values for all soil depths are well below the I_{15max} , 1 in 10 IDF. Thus IOF would prevail. Moreover, even under grassland at the top of the slope (G1), the deeper soil layers are also more impermeable than the surface layer, inferring that rainfall percolating through the more permeable layer above, will be impeded by the lower K_{fs} corresponding to the 0.15 to 0.25 m layer. Thus the occurrence of subsurface stormflow is likely even under grassland.

Using the *in-situ* K_{fs} measurements for 0.04 to 0.15m depths and modelled IDF values for an I_{15max} 1 in 10 IDF (36 mm hr⁻¹); a conceptual spatial diagram inferring possible areas of infiltration and IOF was generated in ESRI® ArcMap™ 9.3.1 (Fig. 10). Areas showing 0 mm hr⁻¹ runoff (blue points in Fig. 10) infer that the *in-situ* K_{fs} measured at these points are greater than 36 mm hr⁻¹, so all rainfall can infiltrate. When there is IOF, the *in-situ* measured K_{fs} is less than 36 mm hr⁻¹ and at these points the quantity of overland flow depends on how high (or low) is the *in-situ* K_{fs} . Following this concept (Fig. 5 and Fig. 10), the two broadleaf woodland areas (DW1 and DW2) have the greatest capacity to accept high intensity rainfall events, whereas the floodplain (including most of the points in the Wetland woodland, FW4) have the least capacity to infiltrate high intensity rainfall.

Fig. 10: Conceptual diagram of runoff during an I_{15max} 1 in 10 year rainfall event (36 mm hr⁻¹) relating to K_{fs} measured at 0.04 to 0.14 soil depth. When runoff is 0 mm hr⁻¹, the total rainfall will infiltrate because the K_{fs} measured at a point is greater than 36 mm hr⁻¹. If the *in-situ* K_{fs} is less than 36 mm hr⁻¹, a portion of the rainfall will become infiltration excess overland flow and generate runoff. Grid areas are identified as abbreviations and contour lines are shown as black full lines, ranging from 210 m to 260 m. G1 is grazed grassland, DW1 is 500 year old broadleaf woodland G2 is grazed grassland, DW2 is 180 year old broadleaf woodland, G3 is grazed grassland and CW3 is 45 year old conifer plantation FW4 is floodplain woodland and G4 is grazed grassland. DW1, G1 and FW4 are enlarged to show the full variation of K_{fs} spatial variation.

When investigating the deeper soil depths (0.15 to 0.25 m) within the adjacent grassland and woodland areas (G1 and DW1), and using the same concept as discussed in Fig. 10, the lower K_{fs} values at depths 0.15 to 0.25 m in G1 would be impermeable to the high intensity rainfall (36 mm hr⁻¹) that has previously percolated through the upper soil layer (Fig. 11).

Thus both SSF and SOF could occur in the grassland. In contrast, DW1 shows a mosaic of some impermeable deeper areas (at 0.15 – 0.25m.) in combination with other areas of higher K_{fs} . Such circumstances would allow high intensity rainfall to percolate to greater

depths in some parts and concurrently be impeded in others parts of DW1, on the lines highlighted above.

Fig. 11. Conceptual diagram of runoff during $I_{15\max}$ 1 in 10 year rainfall event (36 mm hr^{-1}) relating to K_{fs} measured at 0.15 to 0.25. When runoff is 0 mm hr^{-1} , the total rainfall will infiltrate to deeper depths because the K_{fs} measured at a point is greater than 36 mm hr^{-1} . If the *in-situ* K_{fs} is less than 36 mm hr^{-1} , a portion of the rainfall will become infiltration excess overland flow and generate runoff or subsurface storm flow. The light grey area is grassland (G1) and the dark grey area is 500 year old broadleaf woodland (DW1).

5. DISCUSSION

5.1. Effect of land cover and K_{fs}

Considering that each paired grid is located on the same superficial geology (Fig. 2), the very high K_{fs} values under woodland, which are also highly significant ($P < 0.001$) different from the grassland areas, provides a marked contrast in K_{fs} between these adjacent woodland and grassland pairs. This difference between higher K_{fs} values under woodland can be seen to occur within a relatively short spatial distance (as shown in Fig. 4), where K_{fs} increases in the forest areas (DW1 and DW2) at the boundary line between woodland and grassland. Large differences of K_{fs} between pasture land and broadleaf woodland have also been found in other temperate studies, such as Wales, UK (Marshall *et al.*, 2009) and Mont du Lyonnais, France (Gonzalez-Sosa *et al.*, 2010).

The absence of surface litter layer and a shallow organic horizon in the grazed grassland grid areas (e.g. G1, G2, G3 and G4, as shown in Fig. 7) can be expected when grassland is heavily grazed, because little organic material will be available for incorporation into the soil surface, unlike within the forest areas, which are not grazed. Within the woodland areas, there is an active supply of dead organic material that is retained at the soil surface and subsequently is incorporated into the organic horizon. The topsoil of the grassland areas is

therefore *characterised more by the local superficial geology*. The latter contrasts with the woodland areas, which have a clear biological component, as shown by the topsoil profiles having a clear litter layer and relatively deep organic horizon (Fig. 7 and Table 4).

The moderate correlation of coarse root (> 2 mm) presence and increasing K_{fs} , may indicate that the presence of coarse roots is not necessarily a factor increasing K_{fs} , but rather the roots are part of the biological process within the topsoil that interacts with other biological factors (for example, increased organic matter, bioturbation and mycorrhizal fungi network) that in turn, increase K_{fs} . The deeper organic layer within the topsoil profile under woodland in DW1 and DW2, plus the higher root numbers and diameters, especially under DW1 (Fig. 7), infers that macropores and preferential pathways could be present. These circumstances are likely to cause the significantly higher K_{fs} values under broadleaf woodland. Such evidence corroborates other investigations that have observed preferential flow from irrigated experiments following root conduits below trees (Jost *et al.*, 2012; Schwärzel *et al.*, 2012).

The work has highlighted the significantly lower K_{fs} (median 42 mm hr⁻¹) under the conifer plantation (CW3) when compared to the other broadleaf woodland areas ($P < 0.001$). The similarity of K_{fs} in grassland and woodland in Site 3 (as shown in Fig. 5) is probably due to the higher gravel content at Site 3 causing higher K_{fs} under grassland (G3). However, it is surprising that K_{fs} under the conifer plantation (CW3) is low considering that root number and diameter under CW3 is similar to the 180 year old broadleaf forest (DW2), as is shown in Fig. 7. In CW3, the mean standard error (SE) for K_{fs} values was higher than the adjacent grassland area (G3) and it is possible that the litter layer, which was predominantly *P. sylvestris* needles, provided organic colloids (Table 4), which is likely to enhance illuviation in the topsoil areas and reduce soil permeability. Evidence of such a process has been

described under *Picea sitchensis*, in Wales, UK (Chappell, 1996). The soil surface under conifer- dominated forests in north-western USA have also been found to have a 'natural background' water repellency (WDPT >5 s) on air-dry samples (Doerr et al., 2009).

The variance of K_{fs} in the floodplain woodland (FW4) was also not equal to any other woodland area, because it had two unusually high outlier values (247 and 178 mm hr⁻¹, as shown in Fig. 5). In both cases it was observed that the auger holes where these high K_{fs} values were measured had coarse diameter roots. Otherwise the auger holes were dominated by compacted silt and clays, a situation more in common with the floodplain occupied by grassland. Consequently much lower K_{fs} values (median 1 mm hr⁻¹ under grassland and median 8 mm hr⁻¹ under woodland) occur in the floodplain when no coarse roots (> 2mm diameter) are present. The shallow root depths under *Salix caprea* (in FW4) is typical when soils are water logged and soil aeration can at times be minimal for root survival (Jackson and Attwood, 1996). The net result is a heterogeneous root distribution.

5.2. Effect of superficial geology and K_{fs}

The superficial geology survey illustrates the complex geomorphology of the study site that has been developed on a confluence between the Fairy Dean Burn and the main tributary being the Eddleston Water (Fig. 2). Although these rivers are today relatively small, the effects of glaciation and fluvial transport are the major drivers that have deposited and sorted the diverse textural content from clay, silt, sand and gravel within the hillslope and floodplain of this area. Considering, MacDonald et al.'s (2012) conclusion, that "permeability of superficial deposits is most strongly related to the finest fraction", the K_{fs} results for each site under grassland can be compared to presence of fine material (shown in Fig. 8). For example, the highly significantly lower K_{fs} values (i.e. median 1 mm hr⁻¹) measured in the grassland areas in the floodplain (G4), could be attributed to the dominant clay and silt

particle size (shown in Fig. 8), derived from Alluvium soils (Fig. 2). Site 1 (G1) on the other hand was least dominated by the finest fraction and had significantly higher K_{fs} values (median 39 mm hr⁻¹) than any other grassland area.

Soils that have been subjected to glacial processes in Scotland, associated with different superficial geological units, have been observed to have a wide range of K_{fs} , using the Guelph permeameter (Elrick et al., 1989). For example, Lilly (2000) measured a range of K_{fs} values from 0.025 to 432 mm hr⁻¹ for sub-soils under permanent grassland and cultivated fields and MacDonald *et al.* (2012) measured sub-soil K_{fs} ranging from 0.042 mm hr⁻¹ to > 1667 mm hr⁻¹ of *in-situ* material from sub-soils comprising mainly of glacial material.

5.3. Possible stormflow pathways under tree and grass cover

Because the K_{fs} at 0.04 to 0.15 m depth under broadleaf woodlands (DW1 and DW2) exceed the I_{15max} , 1 in 100 IDF, these wooded areas are more likely to act as a 'sink' (i.e., infiltration-vertical percolation dominates) to high intensity rainfall (Fig. 5 and Fig. 10). For example, the measurements of surface K_{fs} in the oldest broadleaf forest (DW1), as shown in Fig. 6, provides evidence that the soil surface provides little barrier to high intensity rainfall infiltrating which could percolate to the lower 0.15 m. Below this depth however, the median K_{fs} under broadleaf woodland (DW1) decreased by six fold when compared to K_{fs} measured in the upper soil layer. Such a decrease in permeability within the sub-soil is likely to cause subsurface storm flow, during high intensity rainfall events. Conceptualising spatially the *in-situ* K_{fs} measurements as possible areas for runoff generation (as illustrated in Fig. 10) infers how the different land covers could act as 'sources' of flood-producing overland flow under high intensity rainfall. IOF is most likely to occur on the floodplain and over some grassland areas. The particularly low surface K_{fs} values in the floodplain grassland (i.e., median K_{fs}

range from 1 to 12 mm hr⁻¹, Fig. 5) illustrates that ponding of water in the floodplain is very likely to occur during most rain events.

Spatial differences of K_{fs} at depth, will cause some high intensity rainfall to percolate beyond 0.25 m (as shown in DW1, by the blue dots in Fig. 11). On the other hand, the point measures of relatively lower K_{fs} values between 0.15 to 0.25 m depth will most likely act as impeding layers and could cause subsurface storm flow.

The high stocking densities observed during the summer cause soil surface compaction and possibly also contribute towards the decrease of K_{fs} at the shallow soil depth, 0.04 to 0.15 m soil depth (Fig. 6) (as reviewed in Hamza and Anderson, 2005). Elsewhere decreased K_{fs} was also found to be lower between 0.05 to 0.10 m depth than when compared to a 0.15 to 0.20 m layer on Fragic Pallic soil in New Zealand after cattle grazing during winter (Drewry and Paton, 2005).

5.4. Using woodland for NFM

The aim of using woodland cover as a NFM technique focuses on the ability for trees to accept rainfall with the effect of reducing the quantity of fast stormflow pathways (e.g., IOF, SOF), and its timing on entry of into river tributaries and groundwater aquifers. In turn, the objective is to reduce quickflow and the peak hydrograph response. This investigation indicates that broadleaf woodland cover (as shown by DW1 and DW2) could significantly facilitate soil hydraulic conductivity and may allow high intensity storm rainfall to infiltrate and subsequently percolate into the topsoil. However, not all tree cover significantly increased K_{fs} . Although the conifer plantation (CW3) had a comparatively higher K_{fs} than the adjacent grassland (G3), such differences in absolute values statistically were not significant. There was evidence of illuviation within the topsoil profile, which could be due to the effect of

colloids from the conifer litter which, in turn, decreased K_{fs} . This process has been suggested in other investigations under conifer plantations (e.g. Chappell, 1996).

This investigation suggests that mature broadleaf forest significantly increases rainfall infiltration and could be planted as a means to facilitate the infiltration of heavy rainfall. This raises the practical issue that following tree-planting with broadleaf species, what is the time scale before an organic soil horizon has sufficiently developed to significantly enhance K_{fs} . The two broadleaf tree areas were 500 and 180 years old, while the surrounding grazed grassland areas had existed for at least 250 years. On the other hand, although DW1 is approximately 320 years older than DW2, the higher K_{fs} of DW1 is statistically not significantly different to DW2. Thus there are indications that a significantly older broadleaf forest (greater than 180 years old) will not necessarily significantly increase K_{fs} much more. On the other hand up to ~180 years from planting, a significant increase of K_{fs} will occur during the growth of such broadleaf woodland. Such trends in K_{fs} are much less apparent for the 45 years *P. sylvestris* plantation. To more comprehensively understand if there is a possible threshold of forest age and the development of soil hydraulic conductivity, requires more baseline research to be undertaken under both broadleaf and conifer woodland that are older than 45 years old, but younger than 180 years old.

6. CONCLUSIONS

Overall this study highlights the significant impact of broadleaf woodland on a hillslope that increases K_{fs} in comparison to grassland areas. In particular, K_{fs} under 180 and 500 year old broadleaf forest was found to be respectively 6 and 5 times higher than neighbouring grazed grassland areas on the same superficial geology. This was attributed to the significantly deeper organic layer in the topsoil profile providing greater available water storage and the

presence of coarse roots (>20 mm diameter) creating conduits for preferential flow. On the other hand, the K_{fs} under *P. sylvestris* had only slightly higher K_{fs} values than the adjacent grassland area, and were statistically not significantly different. This result is surprising considering that root numbers and diameter under *P. sylvestris* is similar to the 180 year old broadleaf forest. Causal factors may have been due to enhanced illuviation of available organic colloids from pine needles, which could cause soil repellency, ultimately reducing K_{fs} . The floodplain broadleaf woodland had significantly lower K_{fs} values than the other woodland area, illustrating the problem of poor soil drainage relating to the gley soils in the floodplain. The coarse roots that did exist within the floodplain woodland were shallow and were spatially less extensive (in clumps), but they did provide some high outlying K_{fs} values and an associated large mean variance in this parameter. The low median K_{fs} values at 0.04 to 0.15 m soil depth under all four measured grassland ranged from median 1 to 39 mm hr⁻¹, where the highest K_{fs} values were in head deposits (high gravel content) and the lowest in the alluvium floodplain deposits (higher silt and clay content). The diverse particle size distribution of clay, silt, sand and gravel within the hillslope indicated the significant effect of glaciation and fluvial transport in depositing and sorting which in turn affected the topsoil K_{fs} under grassland. Moreover no coarse roots (>2mm diameter) were observed in the soil profiles in the grass areas. Thus at these sites the superficial geology was a more dominant influence on K_{fs} than biological factors, which were more dominant in broadleaf woodland. Low K_{fs} values in the floodplain were also observed to be influenced by soil compaction caused by high stocking rates. Of all the soil description parameters (total root numbers, number of roots >5 mm, number of roots between 2 and 5 mm, humus depth, stone size, depth of gravel layer), an increase in K_{fs} was determined by regression analysis to be most

associated with total root numbers >2 mm diameter. By contrast no statistical relationship between gravel size and K_{fs} was evident.

Mapping *in-situ* K_{fs} measurements inferred possible areas of sources and sinks for overland flow during high intensity duration rainfall (the example used was $I_{15\max}$ 1 in 10 year rainfall event). A source of overland flow (infiltration-excess and saturation-excess) occurs in most grassland areas and particularly in the floodplain silty soils. Broadleaf woodland areas are likely to act as sinks to overland flow during high intensity rainfall, but at a depth >0.15 m subsurface storm flow is likely to occur.

In terms of NFM, this study suggests that older broadleaf forests on pastoral hillslopes could mitigate local flooding because of the significantly higher infiltration rates and subsoil K_{fs} under these forested areas in contrast to the heavily, grazed grasslands. However, as indicated earlier, such deciduous forests occupy only $\sim 7\%$ of woodland in the Scottish Borders (Anon, 1999) and a paradigm shift in forestation practice in terms of species is thus required.

Acknowledgements

This research is part of the Eddleston Catchment Project – Phase II, which is funded by the Scottish Government. In particular we are grateful to the University of Western Australia for additional funding and equipment for which the field work depended upon. We thank the British Geological Survey for their support during field work. We also thank the Barony Hotel management and the Walker family for allowing us access to their land, Winkston Farm for

their hospitality and Phillip and Murtle Ashmole for very helpful discussions about ancient woodlands.

References

- Alaoui, A., Caduff, U., Gerke, H.H. and Weingartner, R., 2011. Preferential flow effects on infiltration and runoff in grassland and forest soils. *Vadose Zone Journal*, 10 (1), 367-377.
- Anon. (1999). National Inventory of Woodlands and Trees: Scotland - Borders Region, Inventory Report, Forestry Commission, Edinburgh.
- Anon. (1999). National Inventory of Woodlands and Trees: Scotland - Borders Region, Inventory Report, Forestry Commission, Edinburgh.
- Archer, N.A.L., Bonell, M., MacDonald, A.M., Coles, N. 2013. A Constant Well Head Permeameter formula comparison: its significance in the estimation of field saturated hydraulic conductivity in heterogeneous shallow soils within the Scottish Borders. *Hydrology Research*. In Press.
- Ashmole, P. and Tipping, P.W., 2009. The peat core from Rotten Bottom - a unique record of a changing environment. In: M. Ashmole and P. Ashmole (Eds), *The Carrifran Wildwood Story*. Borders Forest Trust, Jedburgh, UK, pp. 76-80.
- Bens, O., Wahl, N.A., Fischer, H. and Hüttl, R.F., 2007. Water infiltration and hydraulic conductivity in sandy cambisols: Impacts of forest transformation on soil hydrological properties. *European Journal of Forest Research*, 126(1): 101-109.
- Beven, K. and Germann, P., 1982. Macropores and water flow in soils. *Water Resources Research*, 18(5): 1311-1325.
- Bonell, M and Williams, J, 1986. The two parameters of the Philip infiltration equation: their properties and spatial and temporal heterogeneity in a Red Earth of tropical semi-arid Queensland. *Journal of Hydrology* 87: 9-31.
- Bonell, M. 2005. Runoff generation in tropical forests, in: Bonell M., Bruijnzeel L.A. (Eds), *Forests Water and People in the Humid Tropics*. International hydrology series. Cambridge University Press: Cambridge, U.K.; 314-406.
- Bonell, M. and Bruijnzeel, L.A., 2005. Hydrological Research for Integrated Land and Water Management, in: Bonell M., Bruijnzeel L.A. (Eds), *Forests, Water and People in the Humid Tropics: Past, Present and Future*. International hydrology series.. Cambridge University Press, Cambridge, UK.
- Bonell, M. Purandara, B. K., Venkatesh, B., Krishnaswamy, J., Acharya, H. A. K. Singh, U.V., Jayakuma, R. and Chappell, N., 2010. The impact of forest use and

- reforestation on soil hydraulic conductivity in the Western Ghats of India: Implications for surface and sub-surface hydrology. *Journal of Hydrology*, 391(1-2): 47-62.
- Bouwer, H., 1966. Rapid field measurement of air entry vlaue and hydraulic conductivity of soil as significant parameters in flow system analysis. *Water Resources Research*, 2(4): 729-738.
- Bown, C.J., & B.M. Shipley. 1982 *Soil Survey of Scotland: South-East Scotland, 1:250 000 Sheet 7*. The Macaulay Institute for Soil Research, Aberdeen, University Press, Aberdeen.
- British Geological Survey, 2011. *Eddleston Water Catchment: Superficial Geology 1:25 000 Scale*. British Geological Survey, Keyworth, Nottingham.
- British Standards Institution, 1999. BS 5930. Code of Practice for Site Investigations, amendment 1., British Standards Institution, London.
- British Standards Insitution, 1990. BS1377 Part 2.
- Brown, C.J. and Shipley, B.M., 1982. *Soil Survey of Scotland: South-East Scotland, 1:250 000 Sheet 7*. The Macaulay Institute for Soil Research, Aberdeen, University Press, Aberdeen.
- Cambardella, C.A. Moorman, T.B., Noval, J.M., Parkin, T.B., Karlen, D.L, Turco, R.F. and Konopaka, A. E., 1994. Field-Scale Variability of Soil Properties in Central Iowa Soils. *Soil Science Society of America Journal*, 58(5): 1501-1511.
- Chandler, K.R. and Chappell, N.A., 2008. Influence of individual oak (*Quercus robur*) trees on saturated hydraulic conductivity. *Forest Ecology and Management*, 256(5): 1222-1229.
- Chappell, N., 1996. Localised impact of Sitka spruce (*Picea sitchensis* (Bong.) Carr.) on soil permeability. *Plant and Soil*, 182(1): 157-169.
- Chappell, N.A., Sherlock, M., Bidin, K., Macdonald, R., Najman, Y., Davies, G., 2007. Runoff processes in Southeast Asia: role of soil, regolith, and rock type. In: Swada, H., Araki, M., Chappell, N.A., LaFrankie, J.V., Shimizu, A. (Eds.), *Forest Environments in the Mekong River Basin*. Springer-Verlag, Tokyo, pp. 3–23.
- Chorley, R.J., 1978. Glossary of terms. in: M.J. Kirkby (Ed.), *Hillslope Hydrology*. Wiley, Chichester, UK, pp. 365-375.
- Coughlan, K., Cresswell, H. and McKenzie, N. (Eds), 2002. *Soil Physical Measurement and Interpretation for Land Evaluation (Australian Soil and Land Survey Handbooks Series)*. CSIRO Publishing, 392 pp.
- Deuchars S.A, Townend J., Aitkenhead M.J., FitzPatrick E.A. 1999. Changes in soil structure and hydraulic properties in regenerating rain forest. *Soil Use and Management* 15(3): 183–187.

- Doerr, S.H., Woods, S.W., Martin, D.A. and Casimiro, M., 2009. 'Natural background' soil water repellency in conifer forests of the north-western USA: Its prediction and relationship to wildfire occurrence. *Journal of Hydrology*, 371(1-4): 12-21.
- Drewry, J.J. and Paton, R.J., 2005. Soil physical quality under cattle grazing of a winter-fed brassica crop. *Australian Journal of Soil Research*, 43(4): 525-531.
- Drigo R, 2004. Trends and Patterns of tropical land use changes, in: Bonell M, Bruijnzeel LA (eds) *Forests, water and people in the humid tropics: past, present and future hydrological research for integrated land and water management*. International hydrology series. Cambridge University Press, Cambridge, 9–39pp.
- Drigo R, 2006. Overview of land cover change in tropical regions. in: Demuth, S, Gustard A, Planos E, Scatena F, Servat E (eds) *Climate Variability and Change—Hydrological Impacts*. Proc. International 5th FRIEND Conf., Havana, Cuba, IAHS Publication No. 308, 672–678
- Dytham, C., 1999. *Choosing and using statistics*. Blackwell Science, London, Great Britain, 218 pp.
- Elrick, D.E., Reynolds, W.D. and Tan, K.A., 1989. Hydraulic conductivity measurements in the unsaturated zone using improved well analyses. *Ground Water Monitoring Review*, 9(3): 184-193.
- Elsenbeer H., Newton B.E., Dunne T. and De Moraes J.M. 1999. Soil hydraulic conductivities of latosols under pasture, forest and teak in Rondonia, Brazil. *Hydrological Processes* 13(9): 1417–1422.
- Elsenbeer, H., 2001. Hydrologic flowpaths in tropical rainforest soils—A review. *Hydrological Processes*, 15(10): 1751-1759.
- Faulkner, D., 1999. *Flood estimation handbook*. Procedures for flood frequency estimation: Volume 2: Rainfall frequency estimation. Institute of Hydrology, Wallingford, UK.
- Germer, S., Neill, C., Krusche, A.V. and Elsenbeer, H., 2010. Influence of land-use change on near-surface hydrological processes: Undisturbed forest to pasture. *Journal of Hydrology*, 380(3-4), 473-480.
- Ghimire, C.P., Bruijnzeel, L.A., Bonell, M, Coles, N., Lubczynski, M.W. and Gilmour, D.A., 2013. The effects of sustained forest use on hillslope soil hydraulic conductivity in the Middle Mountains of Central Nepal. *Ecohydrology*, On-line 11 February 2013. DOI: 10.1002/eco.1367.

- Gilmour D.A., Bonell M. and Cassells D.S. 1987. The effects of forestation on soil hydraulic properties in the Middle Hills of Nepal: a preliminary assessment. *Mountain Research and Development* 7(3): 239–249.
- Gish, T.J., Starr, J.L., 1983. Temporal variability of infiltration under field conditions. In: Proc. Nat. Conf. on Advances in Infiltration, 12–13 December 1983. Chicago, Ill American Society of Agricultural Engineers. St. Joseph, Mich., pp. 122–131.
- Gonzalez-Sosa, E. Braud, I., Dehotin, J., Lassabatère, L., Angulo-Jaramillo, R., Lagouy, M., Branger, F., Jacqueminet, C., Kermadi, S., Michel, K. 2010. Impact of land use on the hydraulic properties of the topsoil in a small French catchment. *Hydrological Processes*, 24(17): 2382-2399.
- Hamza, M.A., Anderson, W.K., 2005. Soil compaction in cropping systems: a review of the nature, causes and possible solutions. *Soil and Tillage Research* 82, 121–145.
- Hassler, S.K., Zimmermann, B., van Breugel, M., Hall, J.S. and Elsenbeer, H., 2011. Recovery of saturated hydraulic conductivity under secondary succession on former pasture in the humid tropics. *Forest Ecology and Management* 261(10): 1634–1642.
- Hillel, D., 1980. Applications of soil physics. Academic Press, New York.
- Horton RE. 1933. The role of infiltration in the hydrologic cycle. *Transactions, American Geophysical Union*. 14, 446–460
- Hümann, M., Schüler, Müller, C., Schneider, R., Johst, M., Caspari, T., 2011. Identification of runoff processes - The impact of different forest types and soil properties on runoff formation and floods. *Journal of Hydrology*, 409(3-4): 637-649.
- Jackson, M.B. and Attwood, P.A., 1996. Roots of willow (*Salix viminalis* L.) show marked tolerance to oxygen shortage in flooded soils and in solution culture. *Plant and Soil*, 187(1): 37-45.
- Jost, G., Schume, H., Hager, H., Markart, G. and Kohl, B., 2012. A hillslope scale comparison of tree species influence on soil moisture dynamics and runoff processes during intense rainfall. *Journal of Hydrology*, 420-421: 112-124.
- Krishnaswamy, J., Bonell, M., Venkatesh, B., Purandara, B.K., Lele, S., Kiran, M. C.; Reddy, V., Badiger, S. and Rakesh, K. N., 2012. The rain-runoff response of tropical humid forest ecosystems to use and reforestation in the western ghats of India. *Journal of Hydrology*, 472: 216-237.
- Leiva, J.A., Mata, R., Rocha, O.J. and Gutiérrez Soto, M.V., 2009. Chronology of tropical dry forest regeneration in Santa Rosa, Guanacaste, Costa Rica. I. Edaphic

- characteristics. Cronología de la regeneración del bosque tropical seco en Santa Rosa, Guanacaste, Costa Rica. I. Características edáficas, 57(3): 801-815.
- Lilly, A., 2000. The relationship between field-saturated hydraulic conductivity and soil structure: development of class pedotransfer functions. *Soil Use and Management*, 16: 56-60.
- Macaulay Institute for Soil Research., 1984. Organization and Methods of the 1:250 000 soil survey Scotland. *Soil Survey of Scotland*. University Press, Aberdeen, 81 pp.
- MacDonald, A.M., Maurice, L., Dobbs, M.R., Reeves, H.J. and Auton, C.A., 2012. Relating in situ hydraulic conductivity, particle size and relative density of superficial deposits in a heterogeneous catchment. *Journal of Hydrology*, 434-435: 130-141.
- McKay, L.D., Driese, S.G., Smith, K.H. and Vepraskas, M.J., 2005. Hydrogeology and pedology of saprolite formed from sedimentary rock, eastern Tennessee, USA. *Geoderma* 126: 27-45.
- Marshall, M.R., Francis, O.J., Frogbrook, Z.L., Jackson, B.M., McIntyre, N., Reynolds, N., Solloway, I., Wheeler, H.S. and Chell, J., 2009. The impact of upland land management on flooding: Results from an improved pasture hillslope. *Hydrological Processes*, 23(3): 464-475.
- Morales, V.L., Parlange, J.Y. and Steenhuis, T.S., 2010. Are preferential flow paths perpetuated by microbial activity in the soil matrix? A review. *Journal of Hydrology*, 393(1-2): 29-36.
- Nisbet, T. and Broadmeadow, S., 2003. Opportunity mapping for trees and floods, *Forest Research*, Alice Holt Lodge, Farnham, Surrey GU 10 4 LH, UK.
- Nyman, P., Sheridan, G. and Lane, P.N.J., 2010. Synergistic effects of water repellency and macropore flow on the hydraulic conductivity of a burned forest soil, south-east Australia. *Hydrological Processes*, 24(20): 2871-2887.
- Ó Dochartaigh, B.E., MacDonald, A.M., Merritt, J.E., Auton, C.A., Archer, N., Bonell, M., Kuras, O., Raines, M.G., Bonsor, H., Dobbs, M. 2012. Eddleston Water Floodplain Project: Data Report, Climate Change Programme, Open Report OR/12/059. British Geological Survey, Keyworth, Nottingham, UK.
- Peng, S.L., Wu, J. and You, W.H., 2012. Recovery of saturated hydraulic conductivity along a forest successional series from abandoned land to mature, evergreen broad-leaved forest in eastern China. *Soil Research*, 50(4): 257-266.
- Perroux, K.M. and White, I., 1988. Designs for Disc Permeameters. *Soil Science Society of America Journal*, 52(5): 1205-1215.
- Reynolds, W.D., Elrick, D.E. and Clothier, B.E., 1985. The constant head well permeameter: effect of unsaturated flow. *Soil Science*, 139(2): 172-180.

- Reynolds, W.D., Elrick, D.E. and Topp, G.C., 1983. A reexamination of the constant head well permeameter method for measuring saturated hydraulic conductivity above the water table. *Soil Science*, 136(4): 250-268.
- Robinson M., Cognard-Plancq A.L., Cosandey C., David J., Durand P., Fuhrer H.W., Hall R., Hendriques M.O., Marc V., McCarthy R., McDonnell M., Martin C., Nisbet T., O'Dea P., Rodgers M. and Zollner A., 2003. Studies of the impact of forests on peak flows and baseflows: a European perspective. *Forest Ecology Management* 186:85–97.
- Schwärzel, K., Ebermann, S. and Schalling, N., 2012. Evidence of double-funneling effect of beech trees by visualization of flow pathways using dye tracer. *Journal of Hydrology*. 470-471: 184-192.
- Scottish Government, 2009. The Flood Risk Management (Scotland) Act 2009, available at www.legislation.gov.uk :
<http://www.opsi.gov.uk/legislation/scotland/acts2009/asp_20090006_en_1>.
- Sobieraj, J.A., Elsenbeer, H. and Cameron, G. 2004. Scale dependency in spatial patterns of saturated hydraulic conductivity. *Catena*, 55: 49-77.
- Soil Survey of Scotland Staff, 1975. Peebles soil map: Soil Survey of Scotland, systematic soil survey; sheet 24 & part of sheet 32. Scale 1:250 000. Soil Survey of Scotland. Macaulay Institute.
- Talsma, T. and Hallam, P.M., 1980. Hydraulic conductivity measurement of forest catchments. *Australian Journal of Soil Research*, 18(2): 139-148.
- Talsma, T., 1987. Re-evaluation of the well permeameter as a field method for measuring hydraulic conductivity. *Australian Journal of Soil Research*, 25(4): 361-368.
- White, I. and Sully, M.J., 1987. Macroscopic and microscopic capillary length and time scales from field infiltration. *Water Resources Research*, 23: 1514-1522.
- World Reference Bank, IUSS Working Group, 2006. World reference base for soil resources 2006. World Soil Resources Reports No. 103. FAO, Rome.
- Ziegler A.D., Negishi J.N., Sidle R.C., Noguchi S. and Nik A.R., 2006. Impacts of logging disturbance on hillslope saturated hydraulic conductivity in a tropical forest in Peninsular Malaysia. *Catena* 67(2): 89–104.
- Zimmermann, B. and Elsenbeer, H., 2008. Spatial and temporal variability of soil saturated hydraulic conductivity in gradients of disturbance. *Journal of Hydrology*, 361: 78-95.

List of Figures

Fig. 1. Aerial Photo and cross-section of the field study site, showing Site 1 which contains Site 1 grazed grassland (G1) and 500 year old broadleaf woodland (DW1) situated at the top of the slope, site 2 contains grazed grassland (G2) and 180 year old broadleaf woodland (DW2) located on a relatively flat part of the slope, site 3 containing grazed grassland (G3) and 45 year old conifer plantation (CW3) is on the steepest part of the slope and site 4 is located on the floodplain and contains floodplain woodland (FW4) and grazed grassland (G4).

Fig. 2. Superficial geology of study area, showing the eight areas of K_f s measurements. Black lines are 10 m contour lines and open white areas are rock outcrops occurring within 1 m of the soil surface. G1 is grazed grassland, DW1 is 500 year old broadleaf woodland G2 is grazed grassland, DW2 is 180 year old broadleaf woodland, G3 is grazed grassland and CW3 is 45 year old conifer plantation FW4 is floodplain woodland and G4 is grazed grassland.

Fig. 3 Modelled DDF curves using the Flood Estimation Handbook (Faulkner, 1999) aggregating rainfalls over 15 to 360 minute rainfall durations for 2, 5, 10, 20 and 100 year return periods.

Fig. 4. Spatial display of K_f s measured points within each grid area. Grid areas are identified as abbreviations and contour lines are shown as black full lines, ranging from 210 m to 260 m. G1 is grazed grassland, DW1 is 500 year old broadleaf woodland G2 is grazed grassland, DW2 is 180 year old broadleaf woodland, G3 is grazed grassland and CW3 is 45 year old conifer plantation FW4 is floodplain woodland and G4 is grazed grassland. Grid areas G1, DW1 and FW4 are enlarged to show the K_f s categories more clearly.

Fig. 5. Box plots of measured K_{fs} for each field site measured between 0.04 to 0.15 m soil depth. K_{fs} median values are given in the table. The superimposed black and dashed lines I_{15max} rainfall intensity events for selected return periods of 1 in 2 years (22.0 mm hr⁻¹), 1 in 5 years (29.8 mm hr⁻¹), 1 in 10 years (36.3 mm hr⁻¹), 1 in 50 years (56.4 mm hr⁻¹) and 1 in 100 years (68.0 mm hr⁻¹).

Fig. 6. Box plots of measured K_{fs} for DW1, G1 and G4 at three different soil depths: 0 m, 0.04 – 0.15 m, 0.15 – 0.25 m. The superimposed black and dashed lines are I_{15max} rainfall intensity for selected return periods of 1 in 2 years (22.0 mm hr⁻¹), 1 in 10 years (36.3 mm hr⁻¹) and 1 in 100 years (68.0 mm hr⁻¹).

Fig. 7. The graphs in the row labelled 'roots', show the number of coarse roots within a soil profile. The y axis is soil depth (cm) and the x-axis is the number of coarse roots; the black bar indicating average number of roots with diameters between 2 to 5 mm and the grey bars indicating number of roots > 5 mm. Error bars show the standard error for each grid area. The row labelled ' K_{fs} ' shows the K_{fs} (mm hr⁻¹) for each sampled point within each grid. The row labelled 'soil' shows the soil profile from 0 to 0.25 m for grid areas G1, DW1 and G4 and RW1, all other profiles are for soil depths 0 to 0.2 m. The L horizon is fresh annual litter, the F horizon is decomposed litter, H is well decomposed matter under aerobic conditions, A is a mineral horizon incorporating organic matter, B is a mineral horizon and C is a mineral layer of unconsolidated material. The black fragments indicate the depth of coarse gravels.

Fig. 8. Average percentage clay, silt and sand measured for each grid area.

Fig. 9. a) K_{fs} for all auger holes versus number of coarse roots (>2 mm). The linear regression line is: $K_{fs} = 25.94 - 3.434\text{roots} + 1.482 \text{ roots}^2 - 0.03648\text{roots}^3$. $P < 0.001$ and R^2 is

52.2%. b) K_{fs} for all auger holes versus maximum gravel size. No statistical significance ($P = 0.891$ and R^2 is -0.88%).

Fig. 10: Conceptual diagram of runoff during an I_{15max} 1 in 10 year rainfall event (36 mm hr^{-1}) relating to K_{fs} measured at 0.04 to 0.14 soil depth. When runoff is 0 mm hr^{-1} , the total rainfall will infiltrate because the K_{fs} measured at a point is greater than 36 mm hr^{-1} . If the *in-situ* K_{fs} is less than 36 mm hr^{-1} , a portion of the rainfall will become infiltration excess overland flow and generate runoff. Grid areas are identified as abbreviations and contour lines are shown as black full lines, ranging from 210 m to 260 m. G1 is grazed grassland, DW1 is 500 year old broadleaf woodland G2 is grazed grassland, DW2 is 180 year old broadleaf woodland, G3 is grazed grassland and CW3 is 45 year old conifer plantation FW4 is floodplain woodland and G4 is grazed grassland. DW1, G1 and FW4 are enlarged to show the full variation of K_{fs} spatial variation.

Fig. 11. Conceptual diagram of runoff during I_{15max} 1 in 10 year rainfall event (36 mm hr^{-1}) relating to K_{fs} measured at 0.15 to 0.25. When runoff is 0 mm hr^{-1} , the total rainfall will infiltrate to deeper depths because the K_{fs} measured at a point is greater than 36 mm hr^{-1} . If the *in-situ* K_{fs} is less than 36 mm hr^{-1} , a portion of the rainfall will become infiltration excess overland flow and generate runoff or subsurface storm flow. The light grey area is grassland (G1) and the dark grey area is 500 year old broadleaf woodland (DW1).

List of Tables

Table 1) Site description, grid sampling size, and K_{fs} measurement depths. G1 is site 1 grazed grassland, DW1 is 500 year old broadleaf woodland G2 is site 2 grazed grassland,

DW2 is 180 year old broadleaf woodland, G3 is site 3 grazed grassland and CW3 is 45 year old conifer plantation FW4 is floodplain woodland and G4 is site 4 grazed grassland.

Table 2. Results of the paired t-test and Wilcoxon's test, which compare the differences between the tree and grassland grid areas within each site. SE of mean is the standard error of the mean, *** indicates highly significant differences between the grid areas within each site. G1 is site 1 grazed grassland, DW1 is 500 year old broadleaf woodland G2 is site 2 grazed grassland, DW2 is 180 year old broadleaf woodland, G3 is site 3 grazed grassland and CW3 is 45 year old conifer plantation FW4 is floodplain woodland and G4 is site 4 grazed grassland.

Table 3. Results of one-way ANOVAs, comparing $\log_{10} K_{fs}$ values for different depths for each grid DW1, G1, G4. *** means that the P-value is very highly significant and ** means the P-value is highly significant. The table also includes the mean and standard error (SE) of K_{fs} values for each soil layer. G1 is site 1 grazed grassland, DW1 is 500 year old broadleaf woodland and G4 is site 4 grazed grassland.

Table 4. Generalised soil descriptions and their relationship with the superficial geology for all grid areas.



Figure 1

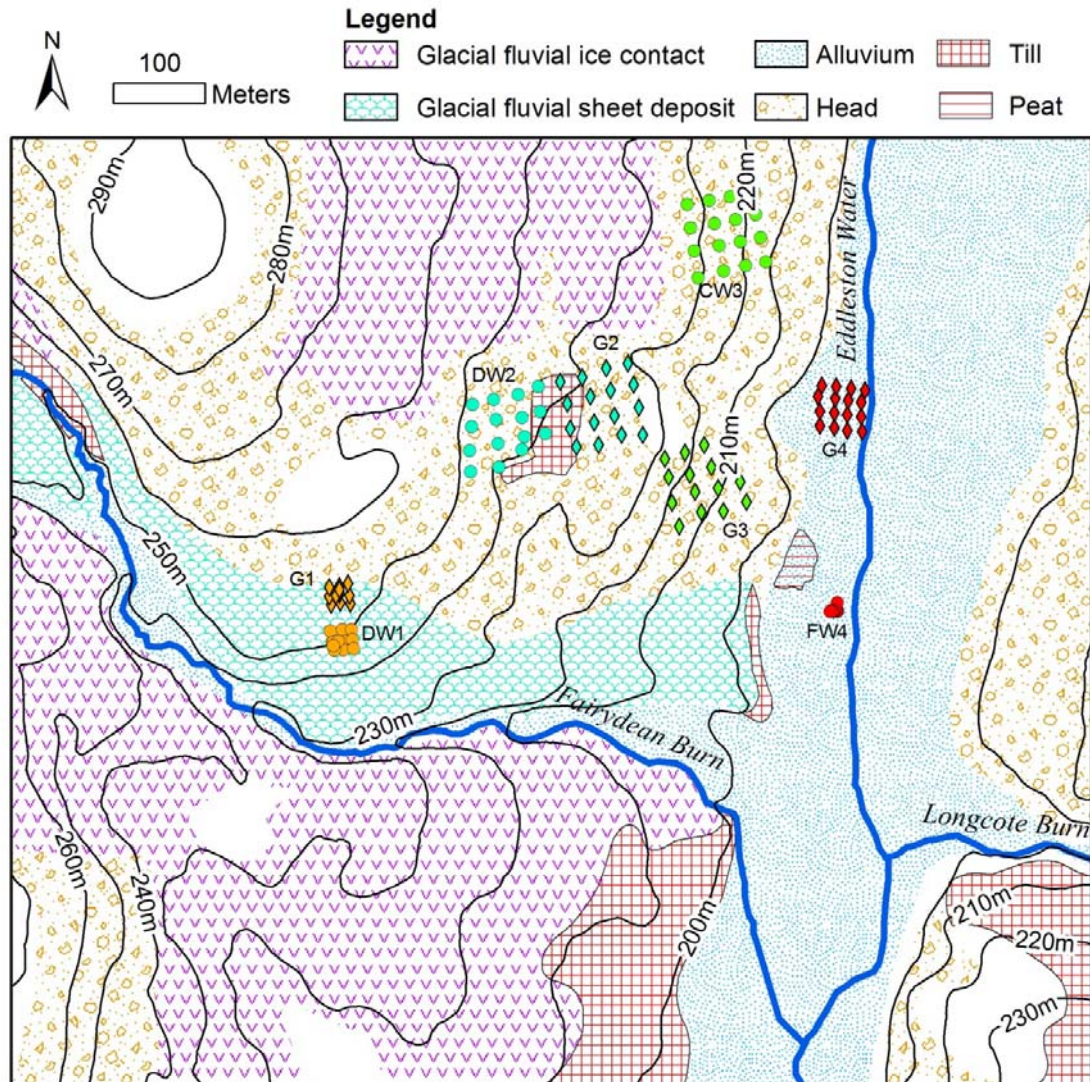


Figure 2

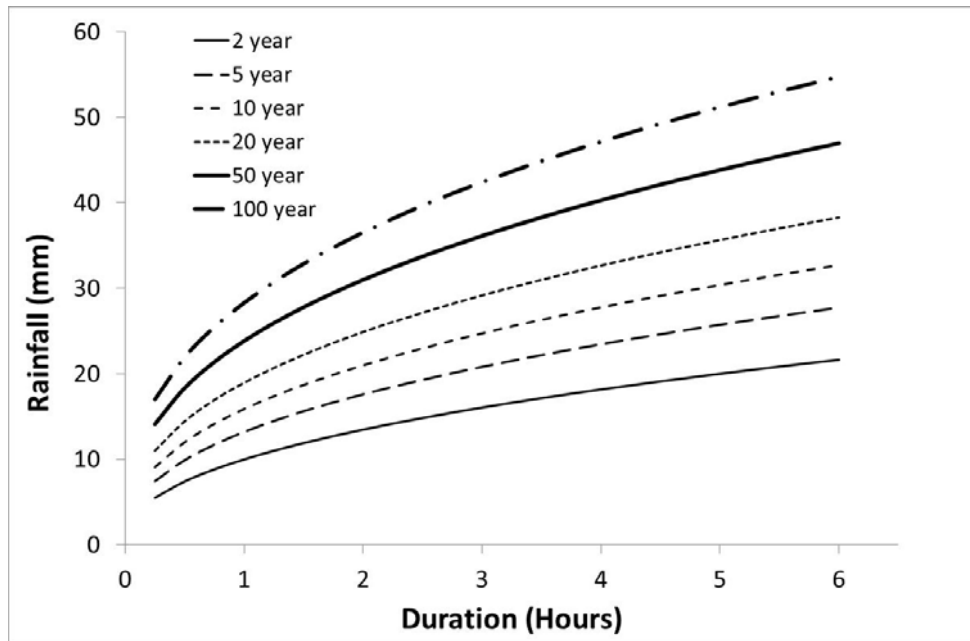


Figure 3

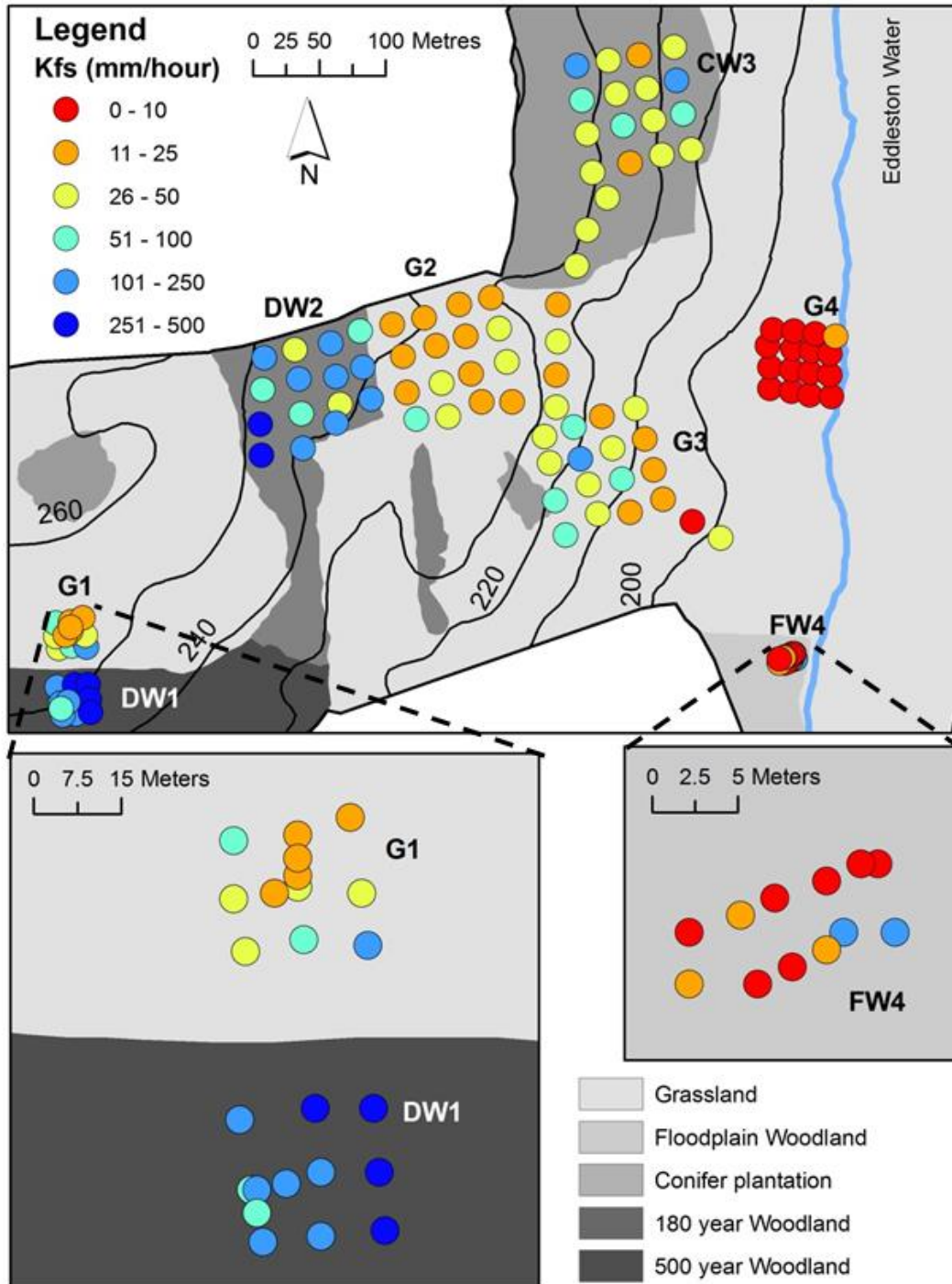


Figure 4

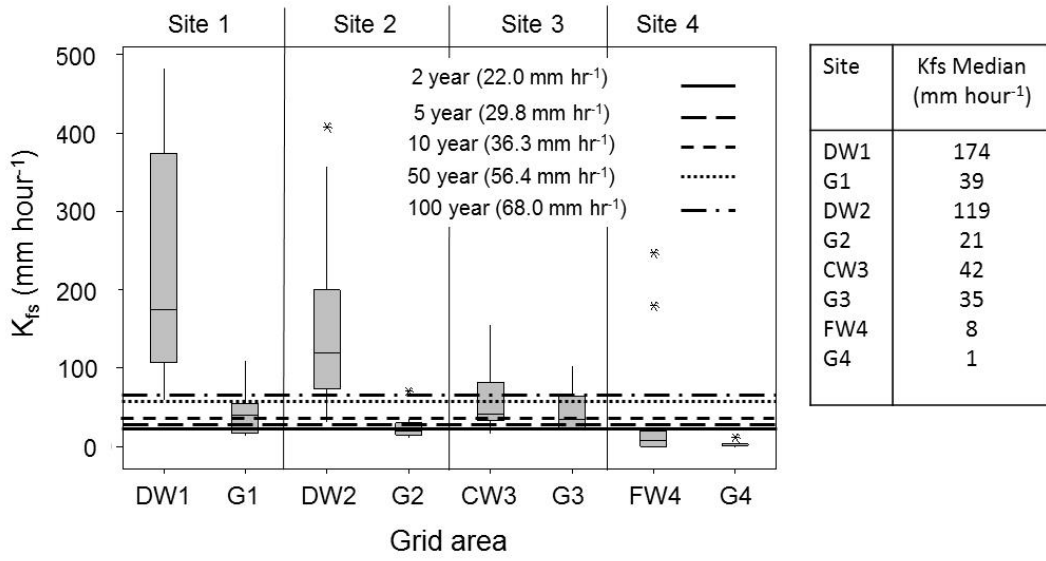


Figure 5

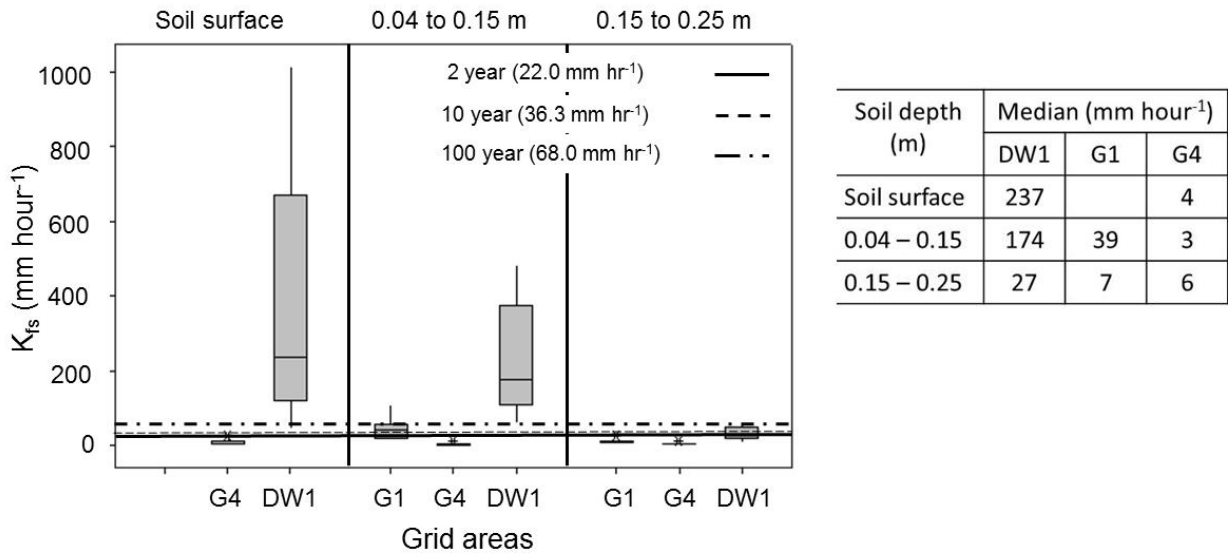


Figure 6

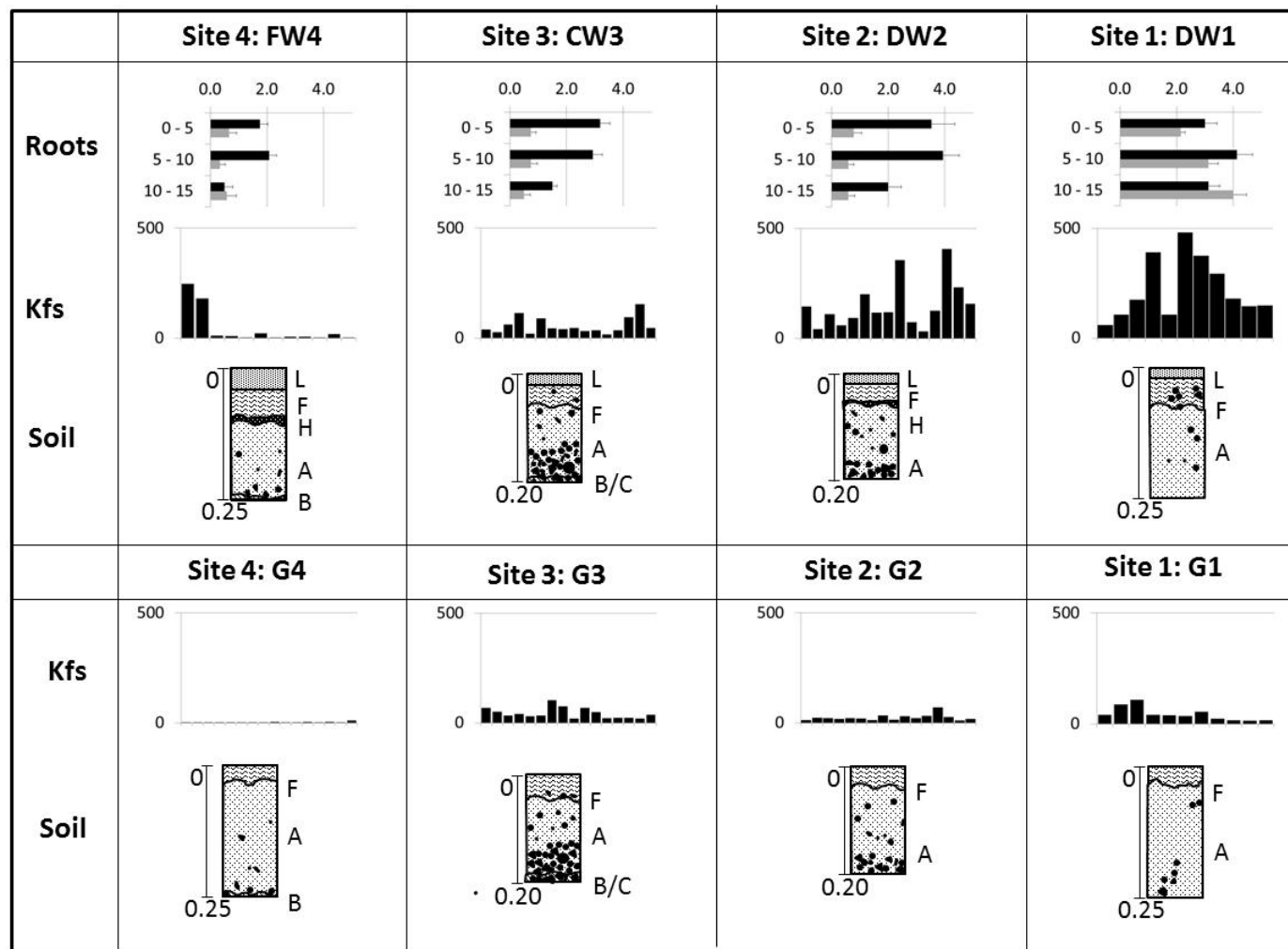


Figure 7

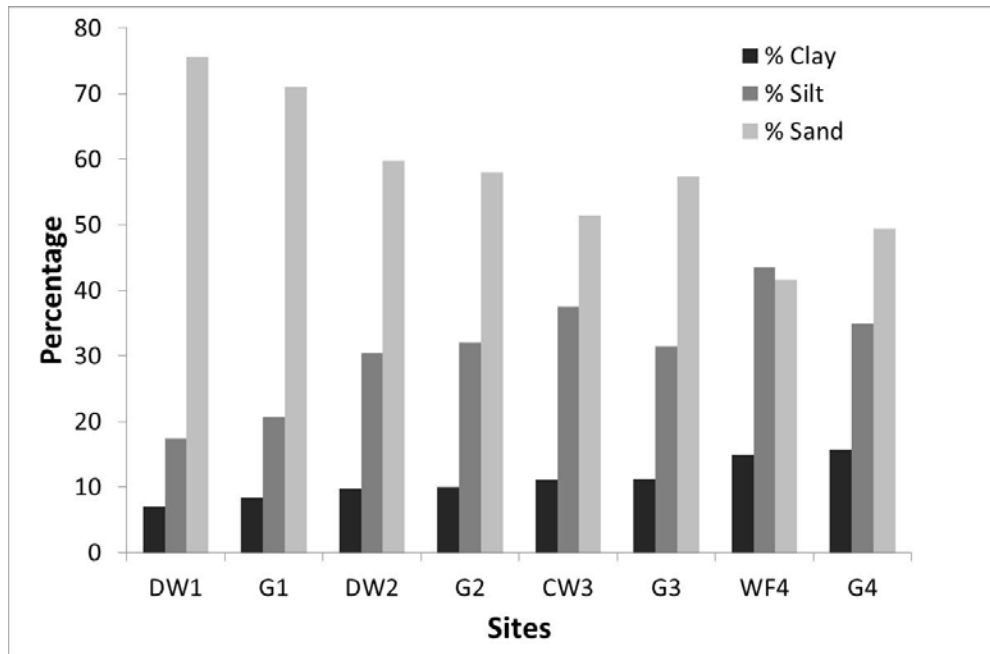


Figure 8

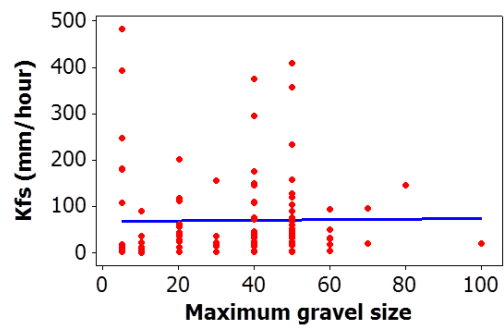
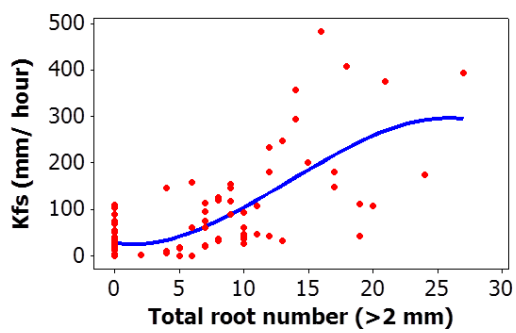


Figure 9

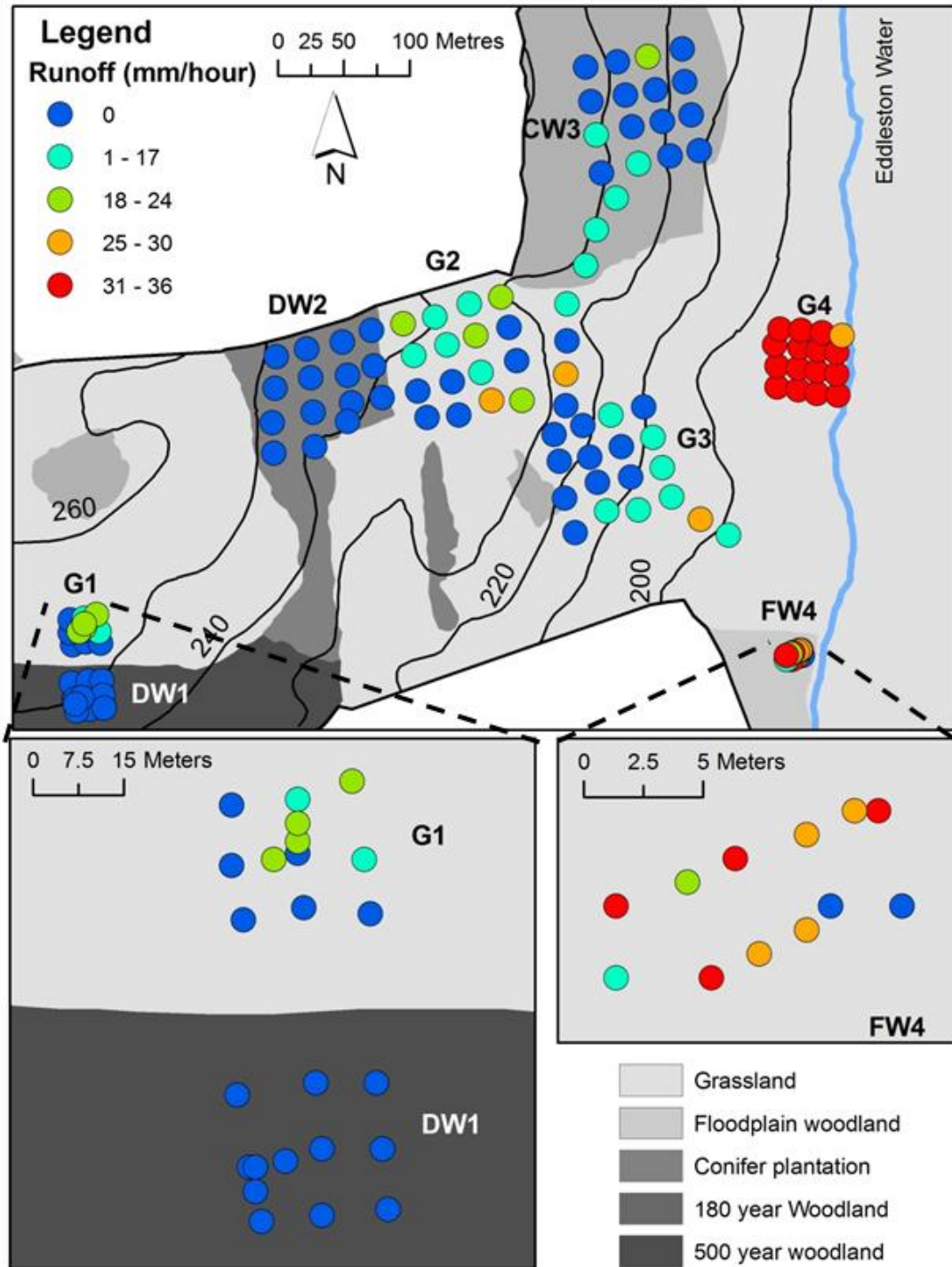


Figure 10

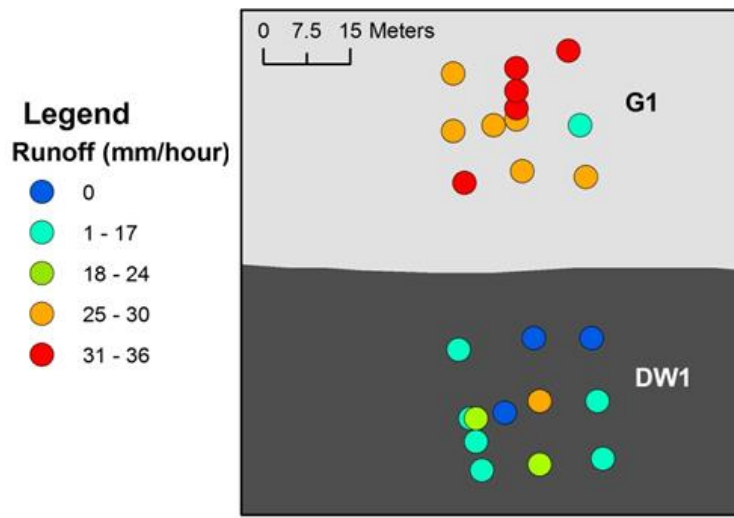


Figure 11

Grid Site	Description	No. of sampled points	Distance between Kfs points (m)	Total size of grid area (m ²)	Depth of augered holes
G1	Improved grassland >265 years	13	10 m	400 m ²	0.04-0.15m, 0.15-0.25m
DW1	Deciduous Woodland, mature Beech > 500 years	15	10 m	400 m ²	0.04-0.15m, 0.15-0.25m
G2	Improved grassland >265 years	16	25 m	5625 m ²	0.04-0.15m
DW2	Deciduous mixed woodland <160 years	15	25 m	5625 m ²	0.04-0.15m
G3	Improved grassland >265 years	16	25 m	5625 m ²	0.04-0.15m
CW3	Conifer plantation 50 years	16	25 m	5625 m ²	0.04-0.15m
G4	Improved grassland >265 years	16	25 m	5625 m ²	0.04-0.15m, 0.15-0.25m
FW4	Deciduous Woodland, mature Willows < 180 years	12	2.5 m	155 m ²	0.04-0.15m

Table 1

Site	Grid area	Mean (mm hr ⁻¹)	Sample number	SE (mm hr ⁻¹)	Statistical test	P-value
1	DW1	224	11	± 41.9	Paired t-test	0.0002***
1	G1	43	11	± 9.2		
2	DW2	152	15	± 28.1	Paired t-test	0.0000***
2	G2	24	15	± 3.7		
3	CW3	56	16	± 9.5	Paired t-test	0.3769
3	G3	43	16	± 6.1		
4	FW4	42	12	± 23.6	Wilcoxon's test	0.004***
4	G4	2	12	± 0.7		

Table 2

Grid area	MS	F- ratio	d.f.	P-value	Soil depth (m)	Mean (mm hr-1)	SE (mm hr-1)
DW1	16.99	27.06	2	<0.001***	Soil surface	407	± 108
					0.04 – 0.15	224	± 41.9
					0.15 – 0.25	30	± 5.21
G1	12.72	35.57	1	<0.001***	0.04 – 0.15	43	± 9.15
					0.15 – 0.25	9	± 1.92
G4	5.02	6.55	2	0.003 **	Soil surface	7	± 2.03
					0.04 – 0.15	3	± 0.69
					0.15 – 0.25	4	± 0.73

Table 3

Grid site	Topsoil Description	Superficial Geology	Soil Association and series
G1 (profiled to 0.30 m)	0 to 0.04 m grass root mat. Silty sand A horizon extends from 0.05 to 0.25 m and grades into a silt/ gravel B Horizon. Gravels exist throughout, but coarse gravel increases in the B horizon below 0.25 m depth.	Glaciofluvial gravel and sand	Ettrick Linhope. Brown Forest soils, freely draining
DW1 (profiled to 0.30 m)	0 to 0.10 m litter layer. Humus layer can be up to 0.05 m. Organic, sandy silt A horizon extends between 0.15 m to 0.30 m and grades into silt/gravel B Horizon. Organic horizons variable depending on distance from trees. Gravels exist throughout, but increase around 0.25 m depth.	Glaciofluvial gravel and sand	Ettrick Linhope. Brown Forest soils, freely draining
G2 (profiled to 0.20 m)	Dense grass root mat 0 to 0.05 m. Silty clay and sandy silt A horizon to 0.20 m. Coarse gravel throughout profile, increasing from 0.20m.	Till occurring within the upper half of the site area. The rest of the area underlain by Head.	Ettrick Kedslie/Linhope Mixed Non-Calcareous gleys, imperfectly draining and brown forest soils, freely draining
DW2 (profiled to 0.20 m)	0 to 0.05 m litter layer. Humus layer variable thickness from 0.01 to 0.05 m. Organic silty clay or sandy silt A horizon extends between 0.10 m to below 0.20 m depth. Organic horizons variable depending	Till occurring within the lower half of the site area. The rest of the area is underlain by Head.	Ettrick Kedslie/Linhope. Mixed Non-Calcareous gleys, imperfectly draining and brown forest soils, freely draining

	on distance from trees. Gravels exist throughout, but increase around 0.20 m.		
G3 (profiled to 0.20 m)	Dense grass root mat 0 to 0.05 m. Silty A horizon extends to around 0.20 m. Coarse gravel throughout profile, increasing at 0.20 m.	Gravels derived from bedrock	Yarrow soils. Brown Forest soils, freely draining
CW3 (profiled to 0.20 m)	0 to 0.05 m litter layer. Dark humus layer variable thickness from 0.01 to 0.05 m. Organic silt A horizon extends from 0.10 m to below 0.15 m and colour changes to red-brown, showing possible illuviation of organic colloids. Cobbles present from 0.15 m grading into a B horizon and in some points reaching a shallow C horizon.	Gravels derived from bedrock	Yarrow soils. Brown Forest soils, freely draining
G4 (profiled to 0.30 m)	0 to 0.04 m organic layer. Clay silt A horizon extends between 0.04 m to below 0.3 m. Gravel occasionally present from 0.2 m. Some gleying below 0.02 m.	Recent riverine alluvial deposits	Alluvial soils, freely to poorly draining
FW4 (profiled to 0.30 m)	0 to 0.08, highly heterogeneous organic layer. Silt A horizon extends from 0.08 m to below 0.3 m. Gleying occurs around 0.015 m soil depth.	Recent riverine alluvial deposits	Alluvial soils, freely to poorly draining

Table 4

Highlights:

We evaluate woodland/grassland cover and soil types to reduce local flooding

We measured field saturated hydraulic conductivity under grassland and woodland

Established broadleaf woodland had significantly higher infiltration rates than grassland

1 in 10 year storm events would cause infiltration-excess overland flow on grassland

We suggest deciduous shelterbelts upslope could locally reduce overland flow